NAVAL FACILITIES ENGINEERING SERVICE CENTER
Port Hueneme, California 93043-4370

Technical Report
TR-2217-SHR

GRAZING-ANGLE FOURIER TRANSFORM INFRARED SPECTROSCOPY FOR SURFACE CLEANLINESS VERIFICATION

Final Report

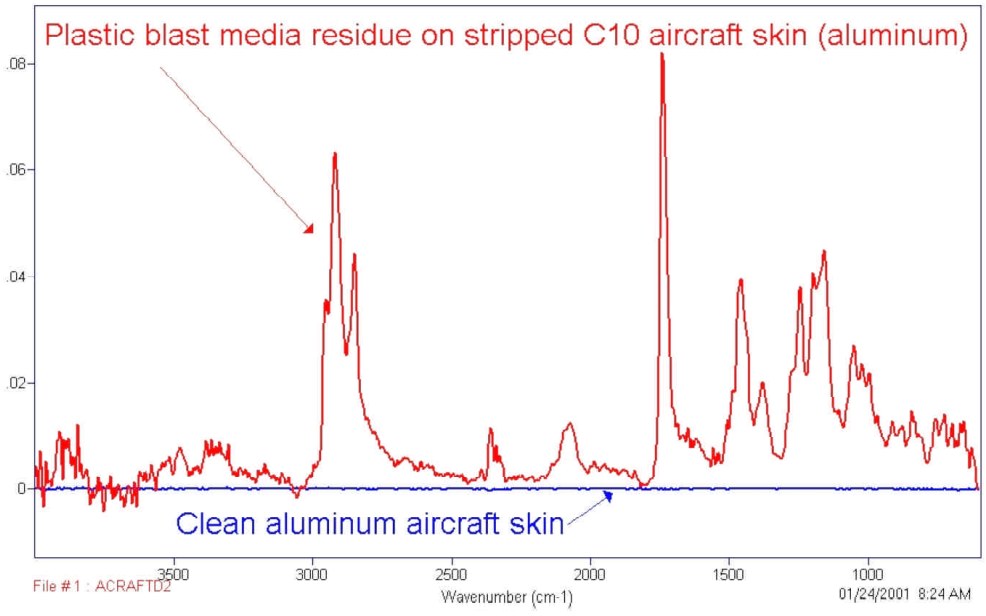

by

Theresa A. Hoffard

March 2003

REPORT DOCUMENTATION PAGE

Form Approved
OMB No. 0704-0188

1. AGENCY USE ONLY (Leave blank)	2. REPORT DATE	3. REPORT TYPE AND DATES COVERED
	March 2003	January 2000 – December 2002

4. TITLE AND SUBTITLE
GRAZING-ANGLE FOURIER TRANSFORM INFRARED SPECTROSCOPY FOR SURFACE CLEANLINESS VERIFICATION – FINAL REPORT

5. FUNDING NUMBERS

6. AUTHOR(S)
Theresa A. Hoffard

7. PERFORMING ORGANIZATION NAME(S) AND ADDRESS(ES)
Commanding Officer
Naval Facilities Engineering Service Center
1100 23rd Ave
Port Hueneme, CA 93043-4370

8. PERFORMING ORGANIZATION REPORT NUMBER
TR-2217-SHR

9. SPONSORING/MONITORING AGENCY NAME(S) AND ADDRESS(ES)
Department of Defense
Strategic Environmental Research and Development Program, Program Office
901 North Stuart Street, Suite 303
Arlington, VA 22203

10. SPONSORING/MONITORING AGENCY

11. SUPPLEMENTARY NOTES

12a. DISTRIBUTION/AVAILABILITY STATEMENT

12b. DISTRIBUTION CODE

13. ABSTRACT (Maximum 200 word

As part of the Surface Cleanliness Verification project, sponsored by the Strategic Environmental Research and Development Program, the Naval Facilities Engineering Service Center conducted an investigation of grazing-angle reflectance Fourier Transform Infrared (FTIR) Spectroscopy as a tool for online cleanliness verification at DOD maintenance and repair facilities. In the project's first year, the feasibility of grazing-angle reflectance FTIR was demonstrated in the laboratory for the detection of organic contaminant residues on reflective surfaces. In Years 2 and 3, this technology was transitioned from the laboratory into a portable field device capable of detecting organic and certain inorganic contaminants on reflective surfaces at very sensitive levels (< 1.0 $\mu g/cm^2$). Examples of DOD applications where surface cleanliness is critical include coating, plating and bonding of aircraft parts; bearing refurbishment; and shipboard surface tile mounting. Visual inspection and water break testing are often inadequate to detect contamination that may cause subsequent bonding or fouling problems if not removed.

14. SUBJECT TERMS	15. NUMBER OF PAGES
FTIR, Fourier transform, infrared, spectroscopy, grazing-angle, reflectance, surface contamination, cleaning verification, NFESC, cleanliness, residue, contaminants, portable	60
	16. PRICE CODE

17. SECURITY CLASSIFICATION OF REPORT	18. SECURITY CLASSIFICATION OF THIS PAGE	19. SECURITY CLASSIFICATION OF ABSTRACT	20. LIMITATION OF ABSTRACT
U	U	U	U

NSN 7540-01-280-5500 Standard Form 298 (Rev. 2-89) Prescribed by ANSI Std Z39-18 298-102

EXECUTIVE SUMMARY

As part of the Surface Cleanliness Verification Project, the Naval Facilities Engineering Service Center (NFESC) conducted a study of grazing-angle reflectance Fourier Transform Infrared (FTIR) Spectroscopy as a tool for on line cleanliness verification at Department of Defense (DOD) cleaning facilities. Examples of applications where surface cleanliness is critical include coating, plating, and bonding of aircraft parts; bearing refurbishment, and shipboard surface mounting of absorbing tiles. In cases such as these, visual inspection or water break testing are often inadequate to detect contamination that will cause subsequent bonding or fouling problems.

NFESC partnered with Sandia National Laboratories, Livermore, California, under the sponsorship of the Strategic Environmental Research and Development Program (SERDP) in the development of two prototype instruments with complementary capabilities for cleaning verification. While Sandia conducted studies on an infrared laser-imaging device, NFESC led the effort to develop grazing-angle reflectance FTIR technology into a real-time, on-site device for post-cleaning determination of surface contamination. In the project's first year, the feasibility of grazing-angle reflectance FTIR was demonstrated in the laboratory for the detection of organic contaminant residues on reflective surfaces. In the project's second and third (final) years, this technology was transitioned from the laboratory into a portable field device capable of detecting organic and certain inorganic contaminants on reflective surfaces.

Results of the study revealed that grazing-angle reflectance FTIR is a very sensitive method for detection of organic residues on metallic surfaces, capable of detecting contaminants to $<1.0\ \mu g/cm^2$ with average baseline noise levels of ≤ 0.0005 reflectance-absorption units on reflective surfaces.

Work during Year 2 of the project included continuation of measurements on calibrated contaminants in the laboratory, designing and constructing the portable grazing-angle reflectance device, and collecting and analyzing DOD hardware samples on both the laboratory and portable devices. During Year 3, the final year of the project, improvements were incorporated into the portable device, corresponding cleanliness verification software was written, and the device was successfully field-demonstrated at selected DOD sites.

TABLE OF CONTENTS

1. INTRODUCTION

As part of the Surface Cleanliness Verification Project, the Naval Facilities Engineering Service Center (NFESC) conducted a study of grazing-angle reflectance Fourier Transform Infrared (FTIR) Spectroscopy as a portable tool for rapid cleanliness verification at Department of Defense (DOD) cleaning facilities.

NFESC partnered with Sandia National Laboratories, Livermore, California, under the sponsorship of the Strategic Environmental Research and Development Program (SERDP) in the development of two prototype instruments with complementary capabilities for cleaning verification. While Sandia conducted studies on an infrared laser-imaging device, NFESC led the effort to develop grazing-angle reflectance FTIR technology into a real-time, on-site device for post-cleaning determination of surface contamination. Surface Optics Corporation (SOC) was selected as the contractor to develop the device.

Applications where surface cleanliness is critical include coating, plating, and bonding of aircraft parts; bearing refurbishment; and shipboard surface mounting of absorbing tiles. In these cases, visual inspection or water break testing are often inadequate to detect contamination that will cause subsequent bonding or fouling problems if not removed.

In the project's first year, the feasibility of grazing-angle reflectance FTIR was demonstrated in the laboratory for the detection of organic contaminant residues on reflective surfaces. During Years 2 and 3, a portable real-time prototype device was successfully designed and built. The device allows process operators to analyze parts on-site and make determinations of subsequent cleaning actions, as well as distinguish between specific contaminants.

The reader is invited to review NFESC Technical Memorandum TM-2335-SHR, *Grazing-Angle Fourier Transform Infrared Spectroscopy for Online Surface Cleanliness Verification: Year 1*, for detailed information on Year 1 laboratory studies (Ref 1).

2. BACKGROUND

The instrumental detection and identification of organic contaminants on reflective surfaces is conveniently and rapidly done by FTIR reflective methods. However, while FTIR is a mature analytical technique, commercially available instrument configurations have not been well suited for real-time analysis of low levels of surface contaminants (<< 1.0 micrometer). Until recent developments in this project, portable infrared devices were limited in sensitivity to surface contaminants by the nature of their optical designs.

FTIR sampling techniques such as attenuated total reflectance (ATR) and diffuse reflectance infrared Fourier transform spectroscopy (DRIFTS) have been commercialized into compact hand-held designs. In these devices, infrared radiation contacts the surface to be analyzed at angles of incidence of near-normal to 60 degrees from normal, resulting in limited sensitivity to very thin layers of surface species.

"Grazing-angle" sampling technology, on the other hand, allows the sensitivity of infrared reflectance measurements to be maximized for thin layers of organic materials on metallic surfaces. As early as the late 1950's, researchers have studied grazing-angle reflectance infrared spectroscopy (Ref 2 and 3). Non-portable, laboratory sampling devices employing grazing-angle reflectance technology are commercially available. Until this joint SERDP project, the technology had not yet advanced to the commercialization of a portable, on-site, and real-time device.

Grazing-angle reflectance theory can be explained by referring to Figure 1. In reflection spectroscopy, a portion of the incident radiation beam (in this case infrared) reflects off the surface of a thin film, while the remaining portion travels (is refracted) through the film and reflects off a reflective substrate back through the film. This is known as "double-pass" reflection-absorption (Refs 4 and 5)

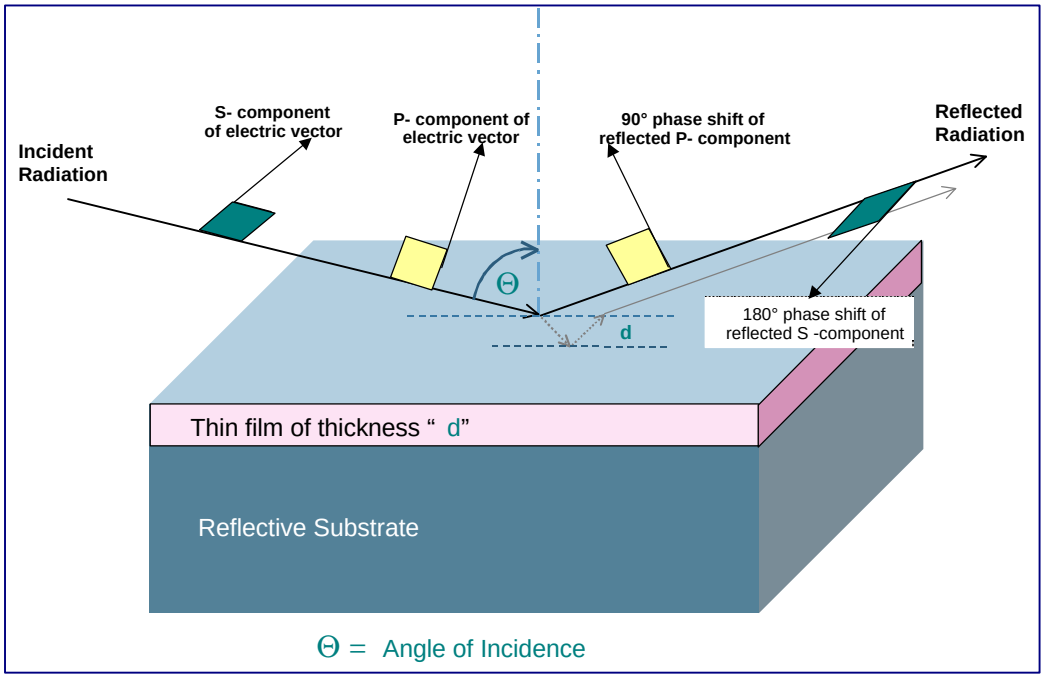

Figure 1. Infrared energy striking a contaminated reflective substrate at a grazing angle of incidence.

Predominantly, improved sensitivity at grazing angles results from the polarization phenomenon of electromagnetic radiation (Refs 6 and 7). The electric vector of all electromagnetic radiation contains two components – the p-component and s-component. For radiation contacting reflective surfaces, the s-component, perpendicular to the plane of reflection (parallel to the plane of the surface), undergoes a phase shift of approximately 180 degrees. The vector sum of the incident and reflected s-component is almost zero at the surface; thus, the two components cancel each other out. At grazing angles, the p-polarized component undergoes a phase shift at the surface from approximately 20 to 180 degrees, depending on the exact angle of incidence. At large incident angles, this phase shift is approximately 90 degrees (Ref 7). The vector sum of the incident and reflected p-component now give an intense electric field oriented perpendicular to the reflecting surface. When passed through a polarizing lens, the s-component of the reflected radiation can be filtered out and only the p-component is detected and converted to a spectrum.

Additionally, at large angles of incidence, the infrared beam contacts the contaminant–laden surface at an increased effective path length through the infrared-absorbing material. In accordance with Beer's Law of absorbance, this enhances the absorption, which results in a stronger FTIR "signal" of the contaminant (Ref 8).

FTIR employs infrared radiation to characterize and quantify organic (and a number of inorganic) materials. At the molecular level, an organic substance absorbs infrared energy and undergoes vibrations at discrete frequencies, or wavelengths, according to its unique chemical makeup. A graph of the energy absorbed versus the infrared frequency in "wavenumbers" (inversely proportional to wavelength) is called the "spectrum" of that material. Unique chemical functional groups produce distinct absorption patterns. For a pure compound, the spectrum becomes a fingerprint of identification. For unknown materials or mixtures such as paints, a spectrum may classify the material as being from a particular chemical family, e.g., a urethane or epoxy. However, it may not always provide enough information to identify the components.

Figure 2 shows a typical reflectance-absorbance FTIR spectrum. The "peaks" or "bands" represent infrared light absorbed by the chemical species being analyzed. The two spectra represent a very thin film of electrically insulating grease on an aluminum substrate analyzed at 0 and 75 degrees (grazing-angle), respectively. The absorbance of the infrared energy in the material is dramatically enhanced at 75 degrees. In the enhanced spectrum, the location and shape of the peaks allow an FTIR analyst to easily classify this material as a silicone.

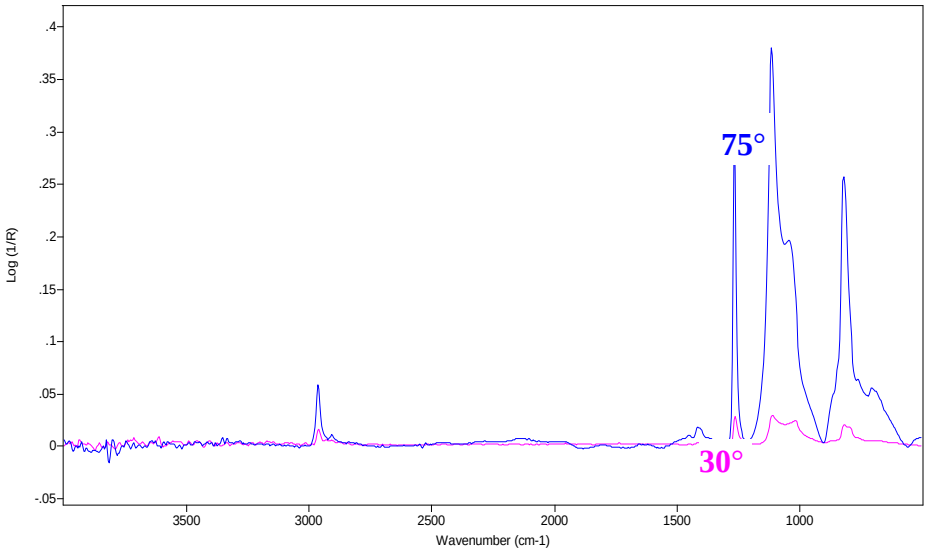

Figure 2. Comparison of a 0.2 μm silicone film on aluminum analyzed at 30°and 75°.

3. EXPERIMENTAL PROCEDURES

Based on results obtained during Year 1, NFESC continued its laboratory experiments on more materials and select "real-world" specimens received from military depots. These laboratory results were then compared to results obtained on the newly developed portable system. The portable system was additionally tested with commercially prepared specimens from the Boeing Corporation. Field demonstrations were conducted with the portable device at two military sites. Based on the results of that demonstration, modifications and upgrades were performed on the system, as well as the development of software specifically designed for cleanliness verification studies. The portable system was taken back to the demonstration site for a second, follow-up test of its new capabilities.

Laboratory analysis was performed on NFESC's Biorad FTS-60 research-grade FTIR utilizing a standard DTGS room-temperature detector. Corresponding background spectra were collected using clean metal substrates at roughness values matching those of the contaminated samples. Background spectra are used to ratio sample and reference "single beam" scans and convert them to reflectance-absorption spectra.

The grazing-angle sampling device used in the laboratory FTIR is commercially available. It is designed for installation inside the sample compartment of a laboratory FTIR, i.e., non-portable operation (Figure 3). This interface is a variable-angle device, allowing analysis of a variety of reflective parts at incident radiation angles of 30 to 80 degrees.

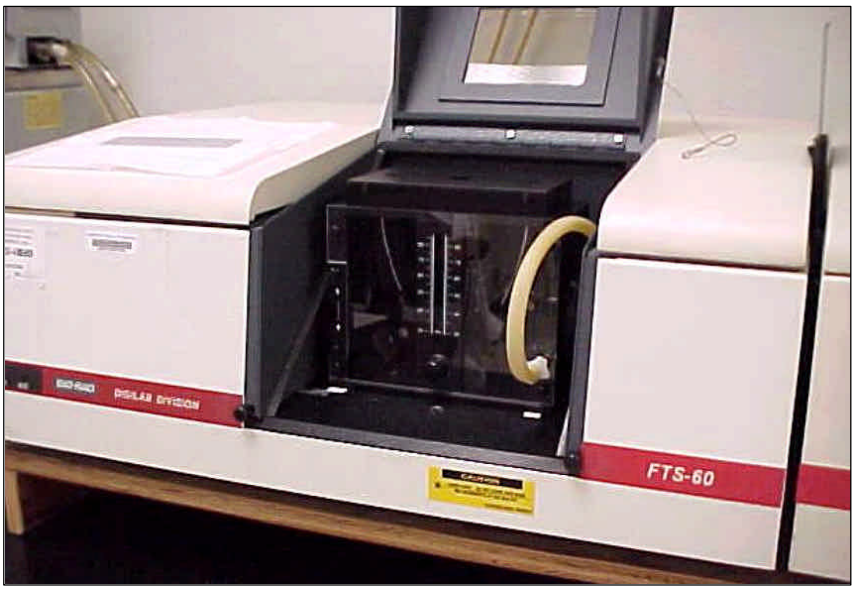

Figure 3. FTIR with variable-angle sampling device.

Appendix A lists all of the test specimens prepared during Years 2 and 3. During Year 1, three contaminants were selected for laboratory examination. During Years 2 and 3, three additional contaminants were tested in the laboratory. The first three contaminants from Year 1, along with these additional contaminants, were used to prepare coupons for testing the portable FTIR device. All contaminants were selected based on feedback from selected military depot installations and DOD contractor facilities. The contaminants are commercially available products used at these facilities. The metal substrates were also chosen based on usage data

obtained from military and contractor facilities. Table 1 shows the contaminants and metal substrates utilized during Years 2 and 3.

Table 1. Years 2 & 3 Laboratory Contaminants and Substrates

Material Designation	Description	Typical Usage
A	White soft solid ester grease	Metal drawing, cutting and lubricating agent
B	Brown liquid – paraffin hydrocarbons	Rust preventative, cleaner, lubricant, protectant for metals
C	Semi-transparent silicone grease	Electrically insulating compound, lubricant
D	Green liquid containing vinyl polymers	Mold-release agent
E	North Island Naval Aviation Depot (NADEP) prepared mixture of hydrocarbons and polyol esters	Individual components used as aircraft engine oil, hydraulic fluid, lubricating greases
F	Hill Air Force Base plastic blast media – methyl methacrylate polymer	Removal of coatings from metal surfaces
Aluminum 7075-T6	1.5” x 5” test panels prepared by commercial vendor at selected roughness values	Aircraft component and framing material
Titanium-4Al-6V	1.5” x 5” test panels prepared by commercial vendor at selected roughness values	Aerospace components
Stainless Steel 304	1.5” x 5” test panels prepared by commercial vendor at selected roughness values	Aerospace components
Steel-C4340	1.5” x 5” test panels prepared by commercial vendor at selected roughness values	High heat applications in aircraft, landing gears
Aluminum 7075	Etched and deoxidized panels provided by North Island NADEP	Aircraft components
Aluminum 2024	Etched and deoxidized panels provided by North Island NADEP	Aircraft components
Aluminum 7075	Chromate conversion coated panels provided by North Island NADEP	Aircraft components
Aluminum 2024	Chromate conversion coated panels provided by North Island NADEP	Aircraft components
Aluminum 2024	Sulfuric acid anodized panels provided by North Island NADEP	Aircraft components
Aluminum 7075	Chromic acid anodized panels provided by Hill AFB, already contaminated	Aircraft components
Aluminum 7075	Dichromate conversion coated panels provided by Hill AFB	Aircraft components

Three surface roughness finishes of commercially milled aluminum test coupons were selected: 80-, 220-, and 600-grit (600-grit being the smoothest). Grit refers to the sandpaper or abrasive blast used by the vendor to create the surface profiles. Two surface roughness levels, 600- and 220-grit, were selected for the remaining commercial metal types. Values were selected as a result of feedback from potential FTIR users at DOD and contractor fabrication and repair facilities. Figure 4 shows varying roughness levels of the aluminum. Figure 5 shows all of the metal types tested.

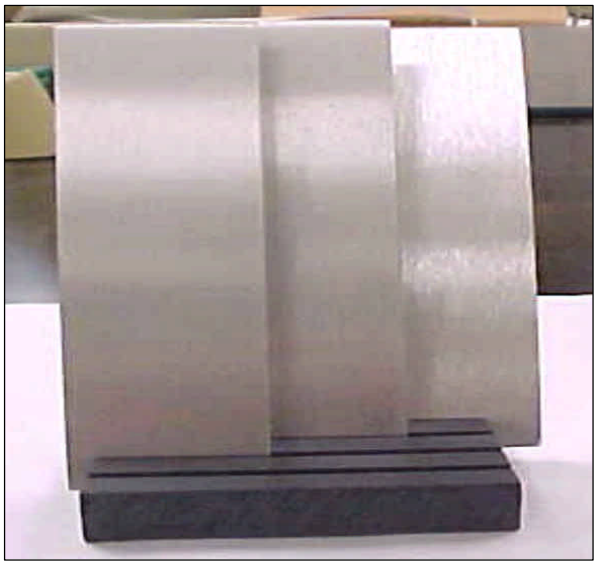

Figure 4. Aluminum surface roughness values 600-, 220-, 80-grit (from left to right).

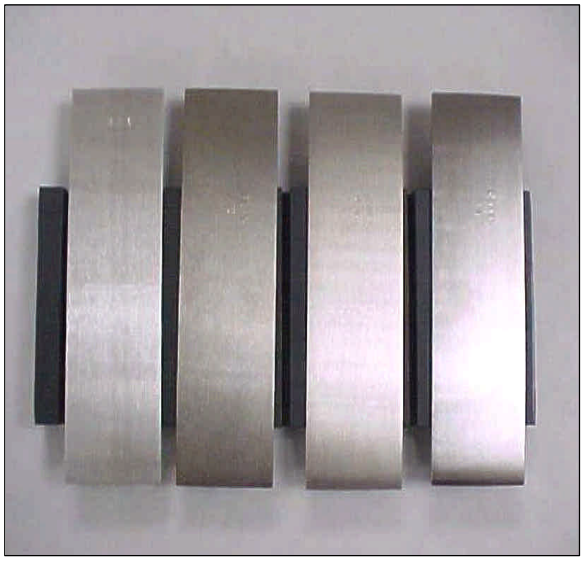

Figure 5. Aluminum, titanium, stainless steel, and steel alloy (from left to right, all at 600-grit).

A profilometer was used to examine the surface roughness profiles and provide "R_a" values (in micrometers or micro-inches) of the commercially obtained coupons. R_a roughness, the arithmetic average roughness, is a term used for machined surfaces. It represents the arithmetic average of the absolute deviations from the mean surface level.

The average surface roughness of aluminum used for aircraft skin is typically required to be = 125 micro-inch (3.175 µm). These metal panels are either sheet metal as-is (rolled, chemically milled, machined), or they are abrasively cleaned by grit blast or sand paper.

Due to the nature of metal shop finishing processes, surface roughness values can vary considerably across a given surface area. The metal surfaces of the coupons, upon finishing at the vendor's facility, acquired a directional "grain" parallel to the coupons' longitudinal axis. Figure 6 shows the variation in surface roughness for the aluminum panels and the relationship to grit finishes. The profilometer data reveal that R_a differences for longitudinal orientation are not as extreme as the differences for transverse orientation.

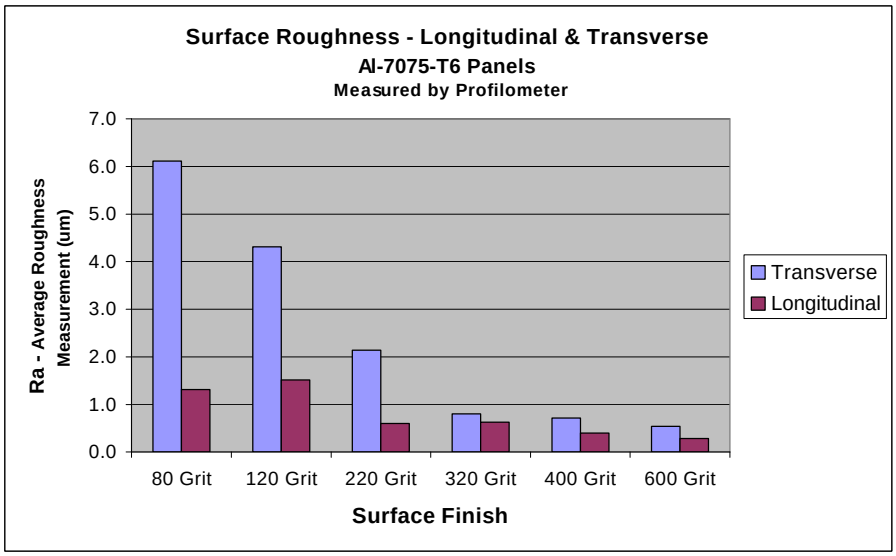

Figure 6. R_a values related to surface finish of test panels.

Except for the panels received from Hill Air Force Base (which were analyzed as-received), all panel coupons where prepared in the laboratory at NFESC, being washed with acetone and cleaned by sonication with a clean-rinsing aqueous cleaner prior to contaminant application. They were thoroughly rinsed and allowed to dry in a desiccator or oven after blotting and air drying. Once dry, they were weighed on a semi-microbalance to the nearest 0.01 mg. Two or more weighings over the course of 2 to 3 days were averaged. No evidence of rusting was seen on the surfaces of the steel C4340 panels that were dried promptly after cleaning.

Contaminants were applied by dilution in appropriate solvents and manual brushing onto the panels (Figure 7). Contaminant D, for example, was diluted in a mixture of water and isopropyl alcohol. Water-only dilutions were found to result in poor wetting of the metal substrates. Alcohol-only dilutions resulted in formation of a solid precipitate from Contaminant D. The combination of water and isopropyl alcohol provided sufficient solvating properties for Contaminant D and adequate wetting of the substrate.

The amount of contaminant applied onto the substrate surfaces was varied by systematically altering the contaminant-to-solvent ratios. The uniformity of the films applied to the substrate test samples varied with physical properties of the contaminants and substrates.

Once contaminated, the panels were allowed to dry under a fume hood to evaporate the solvent. They were then placed in a desiccator for final drying. This served to stabilize the contaminants, allowing for quantification of the contamination film by weighing. Once the weights became stable, final weight averages were recorded. When not being analyzed, the samples were kept in the desiccator.

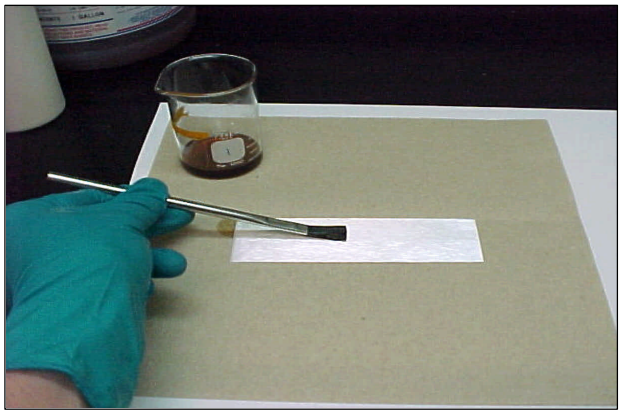

Figure 7. Contaminant being applied to an aluminum panel by manual brushing.

The test coupons were analyzed at NFESC with the laboratory FTIR and grazing-angle reflectance sampling device (Figure 8). Spectra were collected at a 75-degree angle of incidence for all of the specimens, and also at 60 degrees for selected samples. Theoretically, incident angles of 80 to 85 degrees provide the greatest enhancement of the reflectance-absorption signal for metal substrates. However, the configuration of a particular instrument and sampling device optics, as well as the characteristics of the sample may dictate using a smaller angle. It was determined during Year 1 that setting the particular laboratory-sampling device to 80 degrees was increasing baseline noise without significantly enhancing the peak intensities in proportion to the noise. Thus, 75-degree measurements were taken instead of 80- degree measurements.

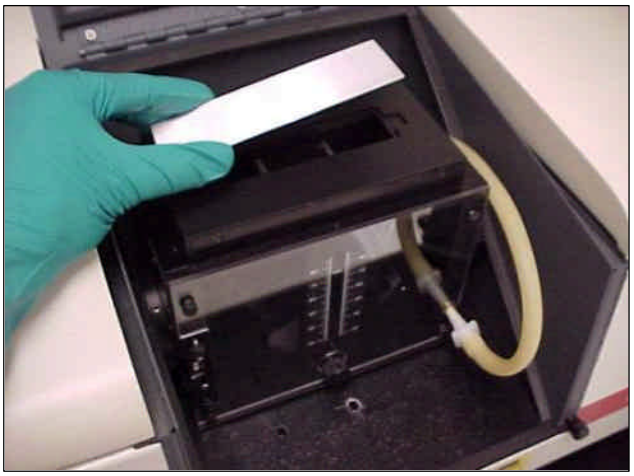

Figure 8. Coupon being placed longitudinally onto sampling device.

Selected test panels were then sent to SOC for analysis on the portable device and the data was compared to data from the non-portable laboratory device. The portable device was designed with a fixed angle of incidence at 75 degrees.

To examine the effect of non-flat sample geometries on the grazing-angle method, six flexible aluminum strips were cleaned, contaminated, and wrapped around 1-cm radius cylinders. These flexible panels were weighed before and after application of Contaminant D. Three of the

strips were roughened with 220-grit sandpaper before the other preparation steps. The remaining strips had a finish that approximating the 600-grit flat aluminum panels. The cylindrical strips were analyzed at NFESC in the same manner as the flat panels (Figure 9).

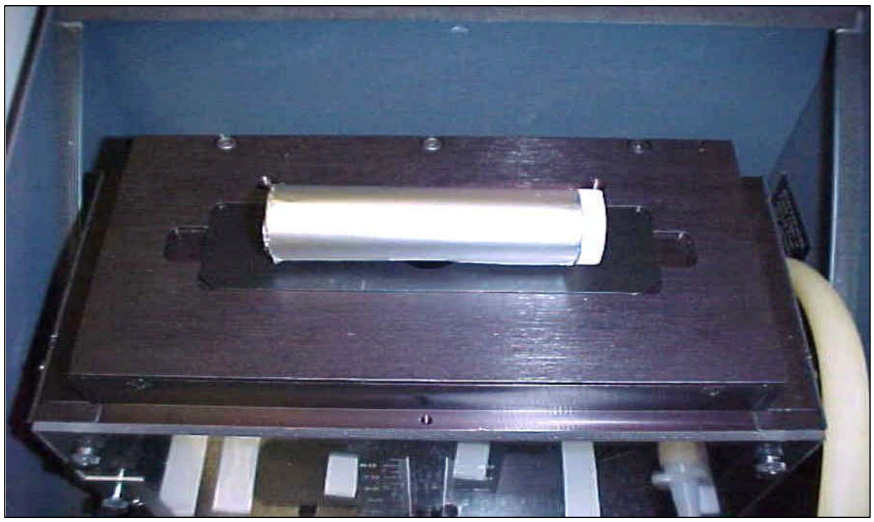

Figure 9. Cylinder being analyzed in a longitudinal orientation.

All test coupons were analyzed using a polarizer in the reflectance device, both laboratory and portable. Figure 10 shows the C-H stretching spectral region of a hydrocarbon contaminant on a vapor-degreased aluminum panel analyzed at 75 degrees with s-polarization, no polarization, and p-polarization of the reflected radiation, respectively. The spectral peaks are enhanced significantly with p-polarization.

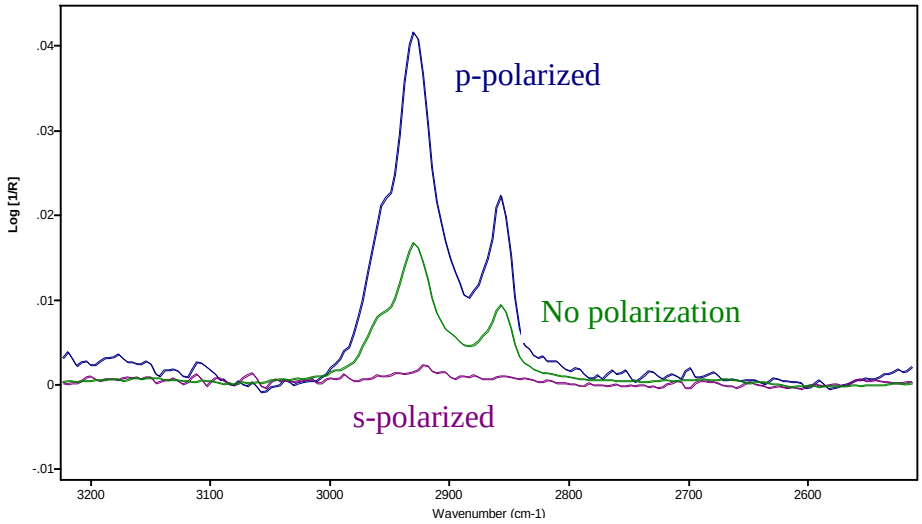

Figure 10. Spectra of a hydrocarbon on vapor degreased aluminum showing the effects of polarization.

Spectral peak area integration calculations were performed by NFESC.

4. RESULTS

A. NFESC Laboratory Analysis of Contaminant D

NFESC TM-2335-SHR contains details of laboratory testing of Contaminants “A”, “B”, and “C” on various metal substrates during Year 1 of the project, and the information will not be repeated here. The laboratory analysis of Contaminant D is presented below.

Figure 11 shows a grazing-angle reflectance spectrum of Contaminant D on an aluminum test coupon (600-grit). For the FTIR analyst, accurate interpretation of the peaks and classification of this film as a vinyl polymer is straightforward because the grazing angle spectrum obtained is intense and clear, even at a film thickness level of < 1 µm. In contrast, other FTIR methods such as diffuse reflectance or specular reflectance would produce much less intense spectra at this level, making it more difficult to accurately classify or quantify the surface contaminant.

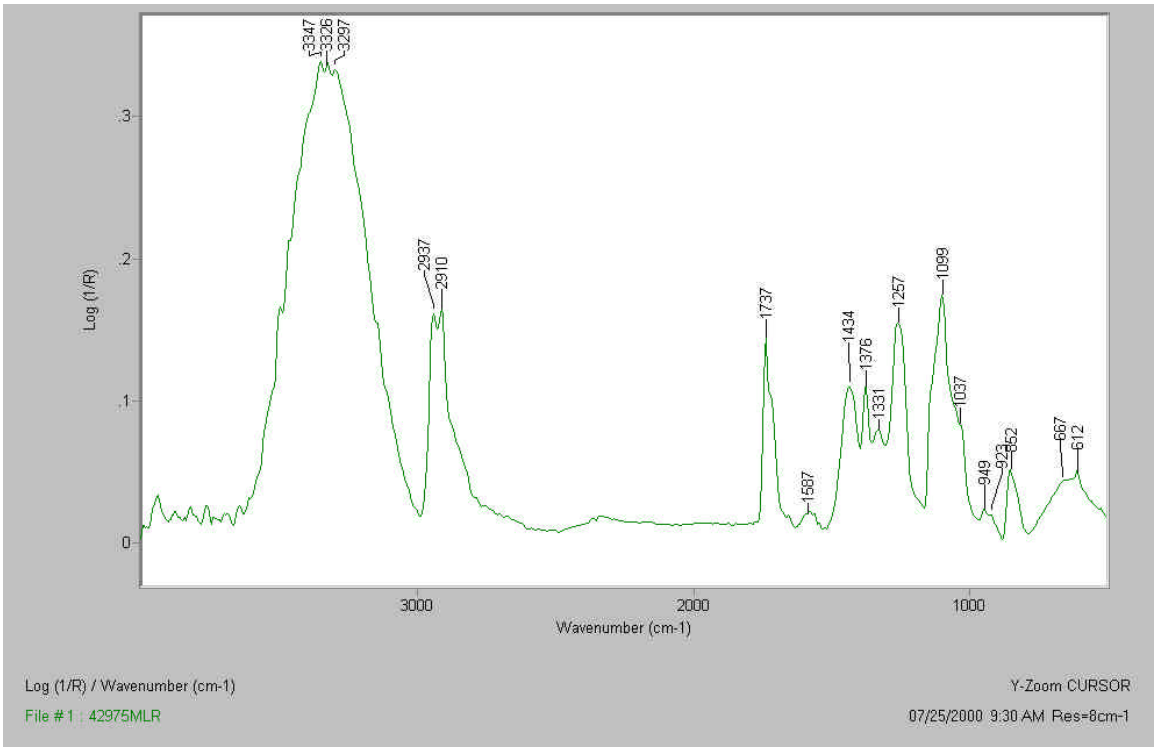

Figure 11. Spectrum of Contaminant D on aluminum coupon (<1.0 µm).

In reflectance FTIR, the log of the inverse-reflectance represents the absorbance of IR energy by the contaminant at various frequencies or wavelengths of infrared light. Selected peak heights or areas under the peaks are linearly proportional to film concentration on the substrate surface. A film concentration level is determined by weighing the substrate coupon before and after application and drying of the contaminant, and dividing the difference by the known area of the coupons. To convert this concentration value to a film thickness value, the concentration value is divided by the specific gravity of the dried contaminant (as determined in the

laboratory). By calculating the film thickness in this manner, an assumption is made that the contaminant is covering the entire surface of the substrate.

Area integration curves of the spectral "carbonyl" peak at 1735 cm^{-1} for three surface roughness values are presented in Figures 12. The integrated areas are plotted against film thickness (calculated as described above). Therefore, each point represents a separate sample coupon.

A surprising degree of non-linearity was observed for the smoothest aluminum coupons, while the 220- and 80-grit panels produced more predictable results. The 600-grit coupons were expected to yield good linearity, and greater peak intensity, since the contaminant is similar in its physical properties to Contaminant B (analyzed during the first year of the project). Both are liquids, soluble in selected solvents, and easy to apply to the metal substrates. It may be that the smoothest surface resulted in the Contaminant D film being distributed less evenly across the surface in contrast to application on the rougher panels. Selected coupons were analyzed at different locations along their lengths and averaged to check for film uniformity. In Figure 12 the vertical error bars indicate similar amounts of variation were observed for the three surface roughness profiles.

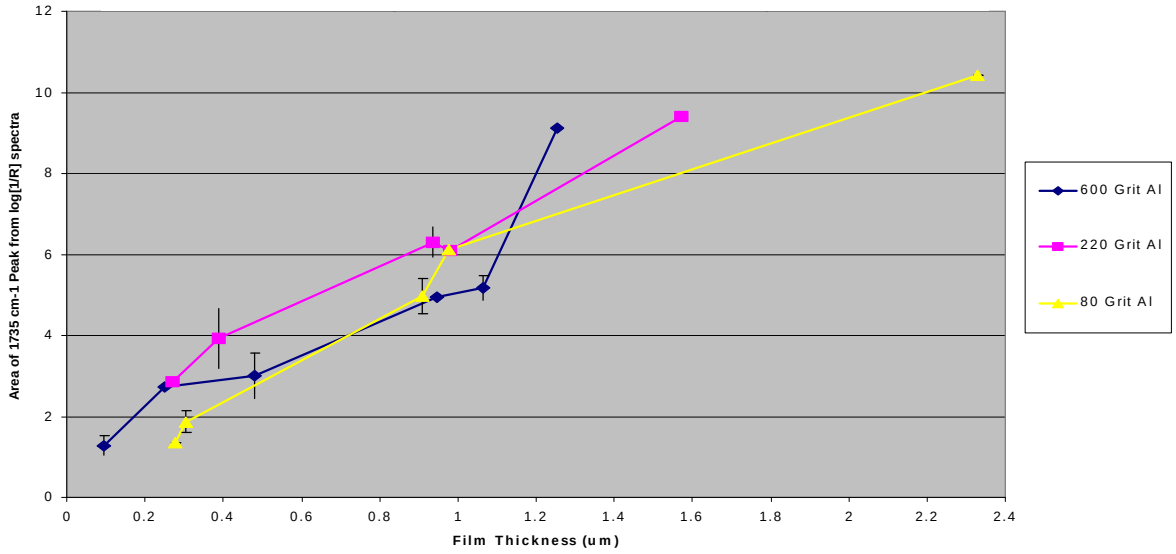

Figure 12. Integrated peak areas of the 1735 cm^{-1} peak in the FTIR reflectance spectra of aluminum panels contaminated with Contaminant D as a function of surface roughness.

Figure 13 shows calibration curves calculated for Contaminant D on metal substrates other than aluminum. As in Figure 12, the peak area of the carbonyl peak (representing the absorbance level of the contaminant proportional to amount of contaminant present) is plotted against the calculated film thickness values. These curves can then be used to quantify the contamination on specimens with unknown levels.

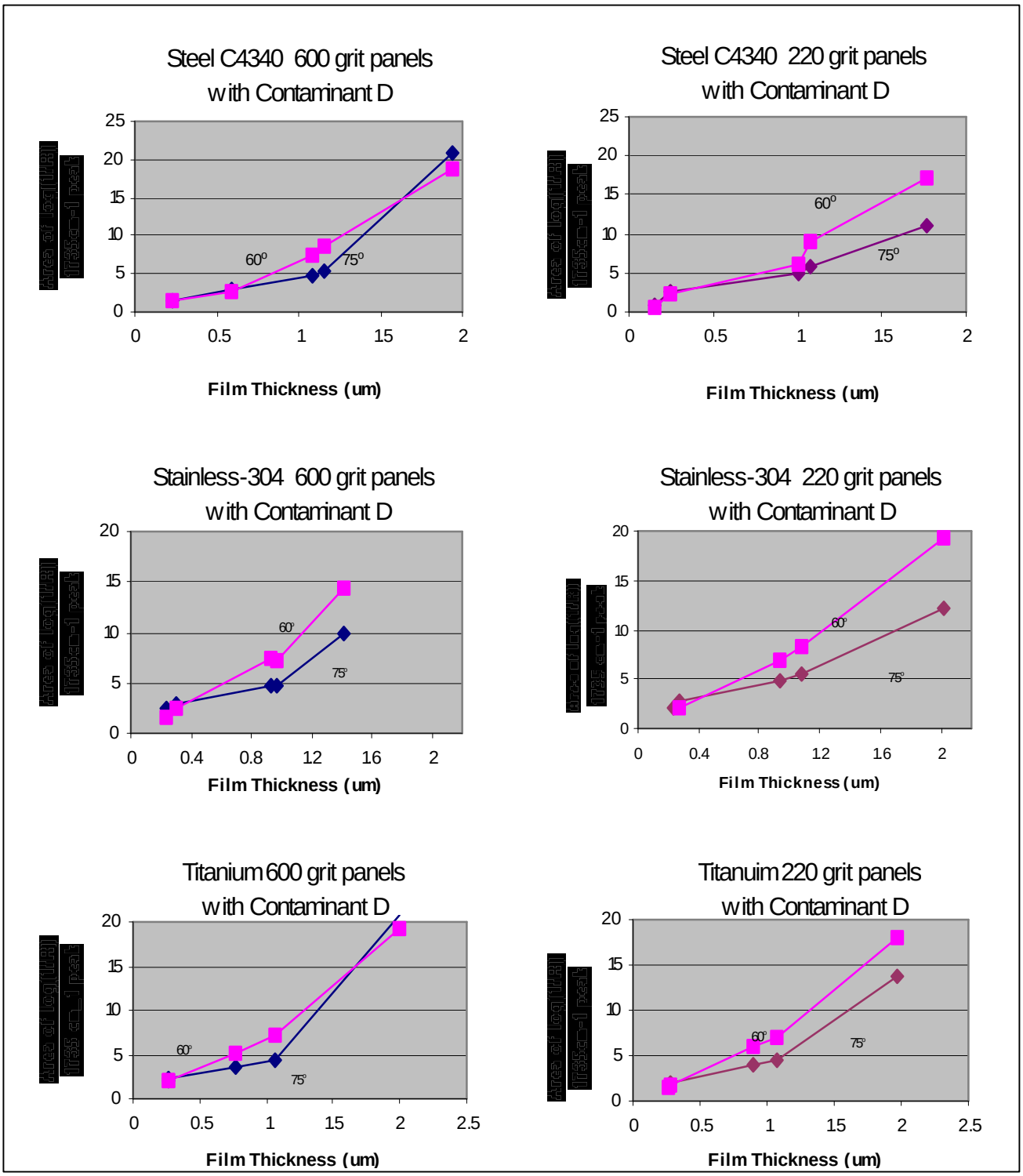

Figure 13. Calibration curves created from calculated spectral peak areas versus film thickness of Contaminant D on three metal substrates with two levels of roughness.

Figure 14 shows calibration curves calculated from spectra taken at 75- and 60-degree angles of incidence for two levels of roughness, 600- and 220-grit on aluminum. As with results obtained during Year 1 with Contaminant A, the intensity of the Contaminant D spectra taken at 60 degrees angle of reflectance was greater than the intensity of the spectra taken at 75 degrees for contaminant levels greater than approximately 0.5 µm. Generally, the higher grazing-angles are expected to produce more intense spectra. However, at optically thick levels, the linearity of the calibration curve breaks down. This behavior is attributed to the morphological and optical characteristics of the contaminant. An accretion of solid residue along the polished grooves of the substrates results in "shadowing" of the illuminated surface. Since the diameter of the focal area of the infrared beam is elongated much more at a 75-degree angle of incidence, it is thus more susceptible to the effects of the shadows.

In contrast to Contaminant A, however, Contaminant D dries to a glossy, relatively smooth finish. Thus, the lessened intensities for the 75-degree analyses were somewhat unexpected. The refractive properties may be interfering with the IR beam's ability to travel through the layer by some other mechanism. Conversely, predictable results are obtained at contaminant thickness values below approximately 0.5 µm. The intensities at 75 degrees exceed those at 60 degrees, as expected.

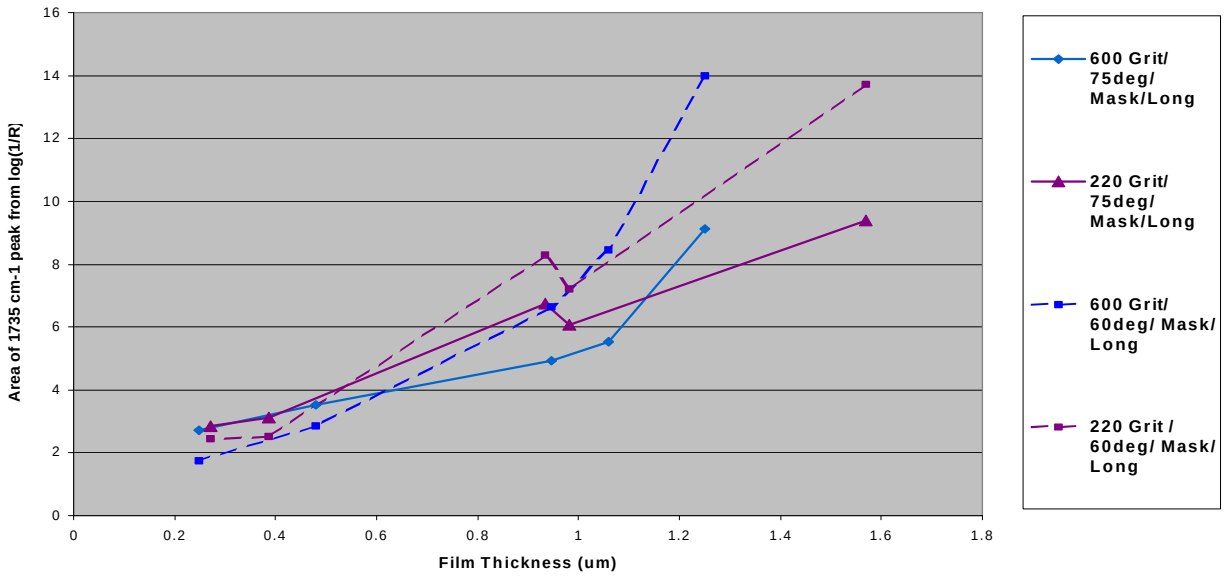

Figure 14. Integrated peak areas of the 1734 cm^{-1} band in the FTIR reflectance spectra of aluminum 7075 panels contaminated with Contaminant D as a function of angle-of-incidence.

For the cylindrical samples, a cross over of intensity is also seen in Figure 15 for the specimens analyzed at 75 versus 60 degrees, just as occurred with the flat specimens (Figure 15). Predictably, the smoother 600-grit cylinders show more intense contaminant peaks for a given film thickness. A predictable nonlinear increase in peak areas is observed for coupons with >1 µm contamination. That is, the grazing angle technique is not as accurate (linear) at levels of contamination above this region.

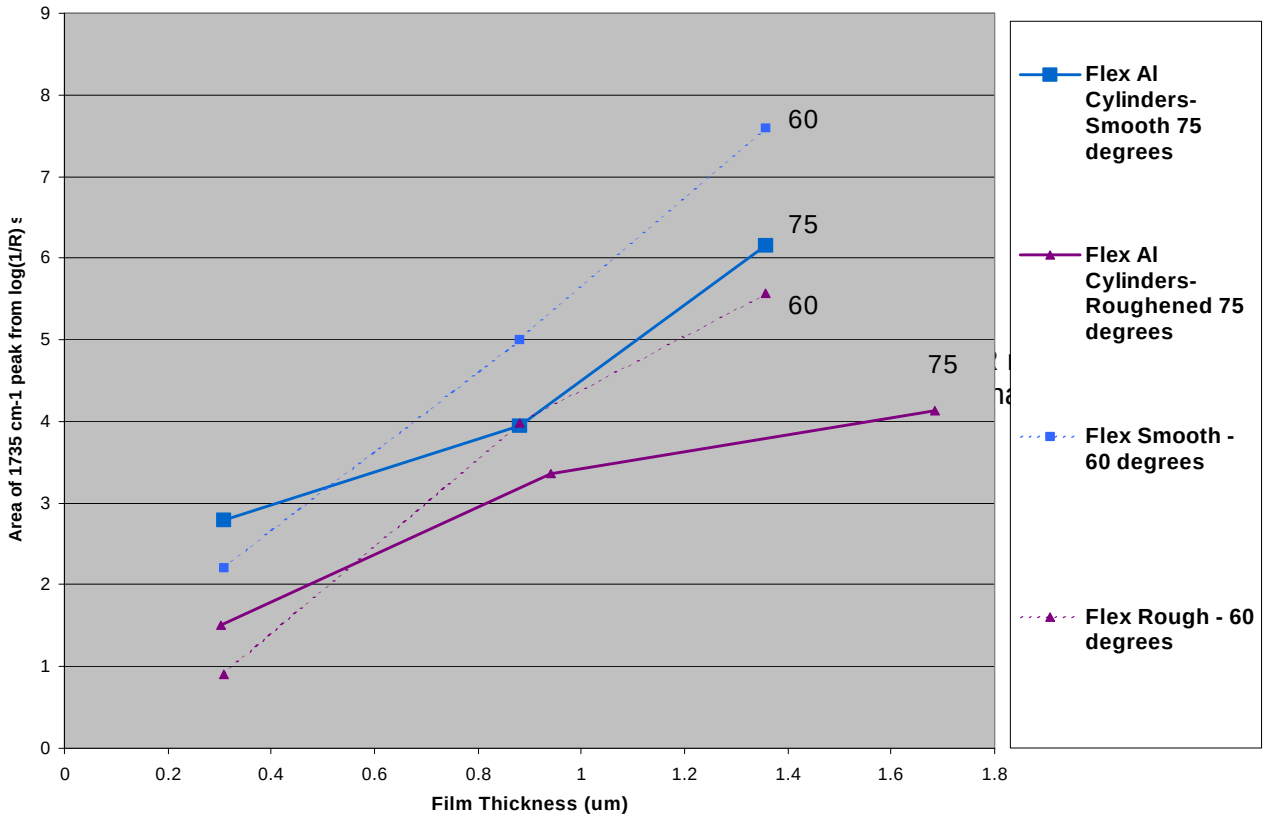

Figure 15. Contaminant D on aluminum cylinders at two angles of incidence and two surface profiles (1-cm radius, longitudinal orientation).

B. Analysis of Non-Metallic Composites

A number of applications at DOD depots and contractor facilities employ non-metallic composite parts. Certain classes of military aircraft contain high percentages of carbon composites on their exteriors.

Organic substrates will absorb infrared radiation and these absorptions are much stronger than the absorbance from the thinner contaminant film. This reduces the overall energy that reaches the FTIR detector and complicates interpretation of the spectra. Also, the optimal angle of incidence varies with substrate type for non-metals and may be below 60 degrees, the grazing angle threshold. Non-metallic surfaces are generally not reflective enough to allow an infrared beam at a grazing-angle to successfully reflect off of the surface and travel to the FTIR detector.

The grazing-angle reflectance device was not expected to provide readable data for contaminants on these types of surfaces. To confirm this, several composite materials were selected and tested in the laboratory grazing-angle FTIR device. These included a vinyl ester fiberglass-reinforced composite, an epoxy fiberglass-reinforced composite, and a carbon fiber vinyl ester composite. Clean flat composite strips were analyzed as reference controls. Strips were then coated with a film of a mixed hydrocarbon contaminant. Spectra of the soiled composites were collected and ratioed against respective clean composite spectra to subtract out absorbance from the plastic substrates.

Figures 16, 17, and 18 show the results of the study. Poor quality spectra were obtained. The energy throughput to the detector was low due to the non-reflective, organic background. This is evidenced by the low log (1/R) values (y axis). Noise, fringe patterns, and "specular reflectance" are evident. Contaminant film concentrations were calculated by weighing to be approximately 300 $\mu g/cm^2$ for the three samples. At this level of contamination, the peaks from the hydrocarbons on a reflective surface would be strong and easily identifiable, especially in the region of 3000 to 2800 cm^{-1}. The sharp bands in the lower wavenumber region, called "Rehstrahlen" peaks, are due to specular reflectance and are not real peaks from the contaminant. The FTIR operator would not be able to identify a contaminant, nor quantify it, from such spectra. The grazing-angle reflectance technique is unsuitable for analyzing organic contaminants on organic composite surfaces.

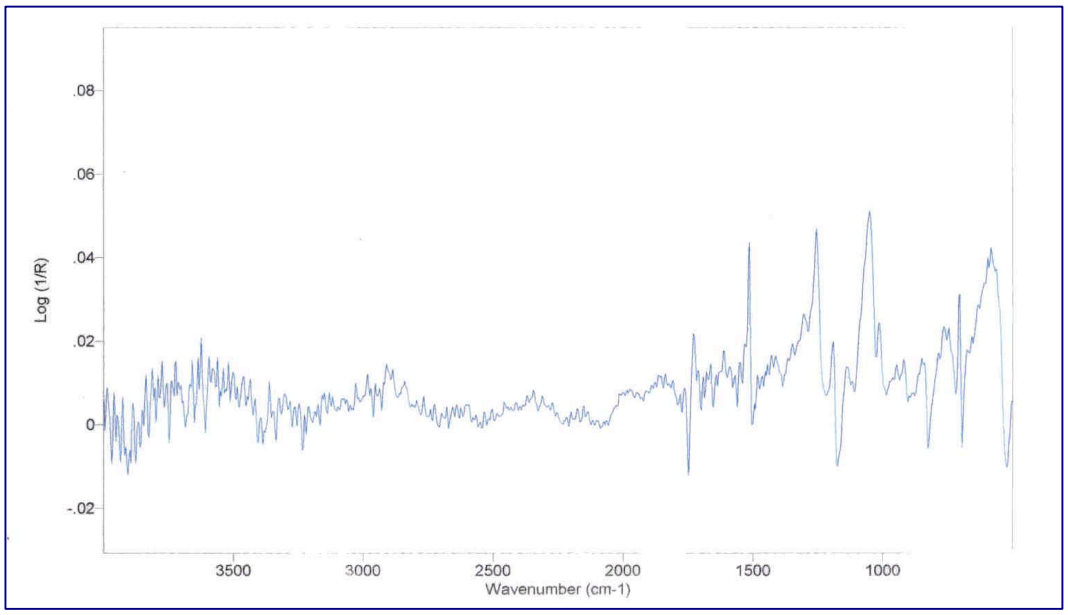

Figure 16. Spectrum of a vinyl ester fiberglass composite soiled with approximately 300 µg/cm^2 hydrocarbon mixture and ratioed against a background spectrum of clean composite.

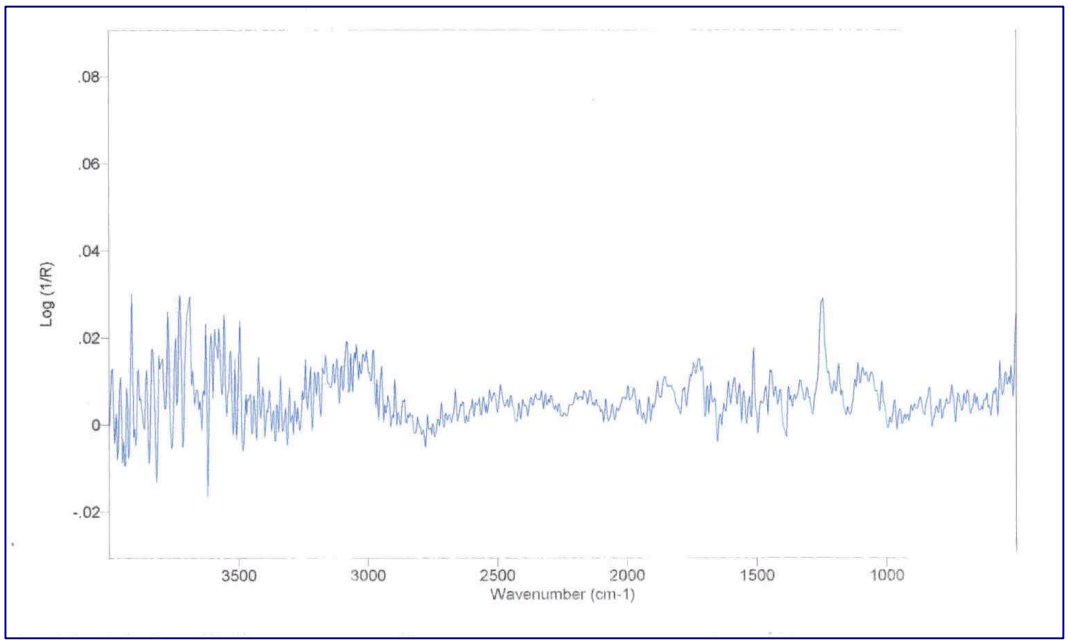

Figure 17. Spectrum of an epoxy fiberglass composite soiled with approximately 290 µg/cm^2 hydrocarbon mixture and ratioed against a background spectrum of clean composite.

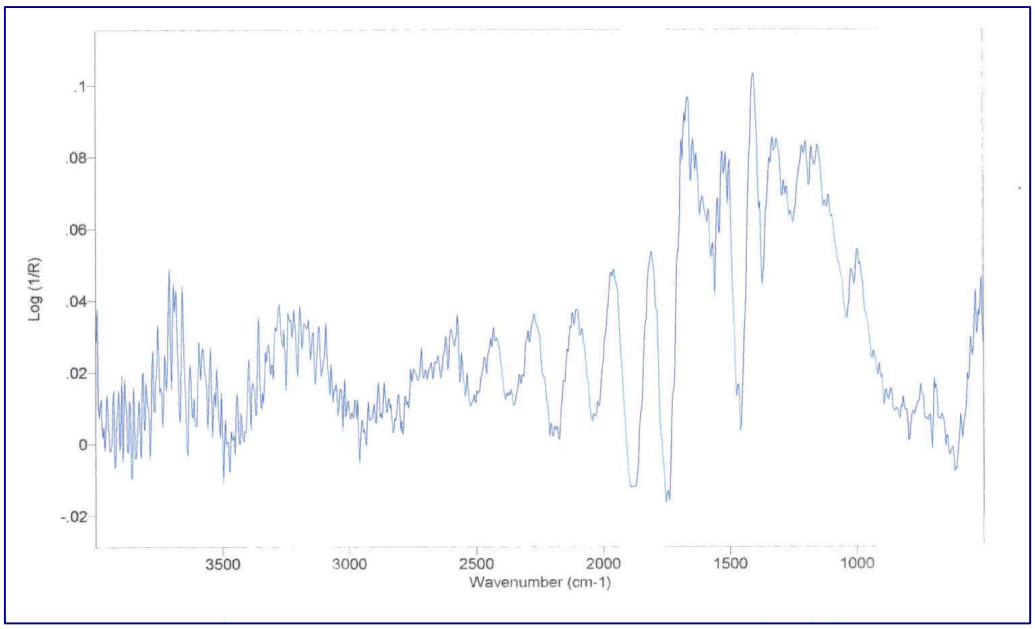

Figure 18. Spectrum of a carbon fiber vinyl ester composite ratioed against a background spectrum of clean carbon fiber vinyl ester composite. A dramatic fringe pattern is evident.

C. Development of the Portable Grazing-Angle Reflectance FTIR

The contract for the development and demonstration of the portable FTIR device was awarded in May 2000 to Surface Optics Corporation (SOC) in San Diego, CA. The design and construction of the grazing-angle reflectance prototype was completed in August 2000, including the construction of a mobile cart for transporting the unit and a swing arm for stable positioning of the unit during analysis. A laptop computer, purge gas supply, and power supply were also included in the prototype package, as shown in Figure 19.

Figure 19. Portable grazing-angle FTIR prototype with computer and cart assembly.

The device is now commercially available from SOC. Several organizations, namely the Boeing Corporation, NASA, and Oak Ridge National Laboratory have purchased units for cleaning verification applications on aircraft, aerospace, and other components.

Based on personnel feedback from initial field demonstrations (see Section E of this report), SOC was awarded a new contract in July 2001 to upgrade the prototype with more user-friendly features. SOC completed the upgrades in January 2002. It was determined that implemented improvements should be those that most enhance the user friendliness of the instrument for shop personnel, and that best serve the demands for DOD cleanliness verification applications. The specific enhancements are:

1. Redesign of a bottom mount for the FTIR optical head so that it can be readily attached to a camera tripod for hands-free analysis of aircraft and similar objects where hand-held operation is not feasible.
2. Development of software dedicated to surface cleanliness analysis that allows operation by persons with minimal knowledge of spectroscopy.

3. Development of a trigger located on the FTIR optical head so that the operator does not need to let go of the device to initiate an analysis at the computer. Previously, the infrared spectrum collection was triggered by pressing a button on the computer several inches or feet away from the FTIR unit. The goal of this improvement was to implement a switch into the spectrometer's handle which, when pressed, initiates the collection of an infrared spectrum. This improvement makes the process a true one-person operation.
4. Development of hardware manuals to allow operation of the device by technicians with minimal knowledge of spectroscopy.
5. Development of software manuals to allow operation of the device by technicians with minimal knowledge of computers and spectroscopy.

The goal of the software development was to allow prediction of surface contamination levels with one click of a remote switch. The recorded spectrum is automatically searched against a spectral library of contaminants (either commercially available or user-specific). The operator has an option to accept the automated selection or browse the library for a more intuitive selection. When the selection is made, an appropriate calibration curve is applied and the contamination level is predicted. The software is Windows-based, and many of the operation functions can be accessed by selecting and pressing icons (Figures 20, 21, 22, 23, and 24).

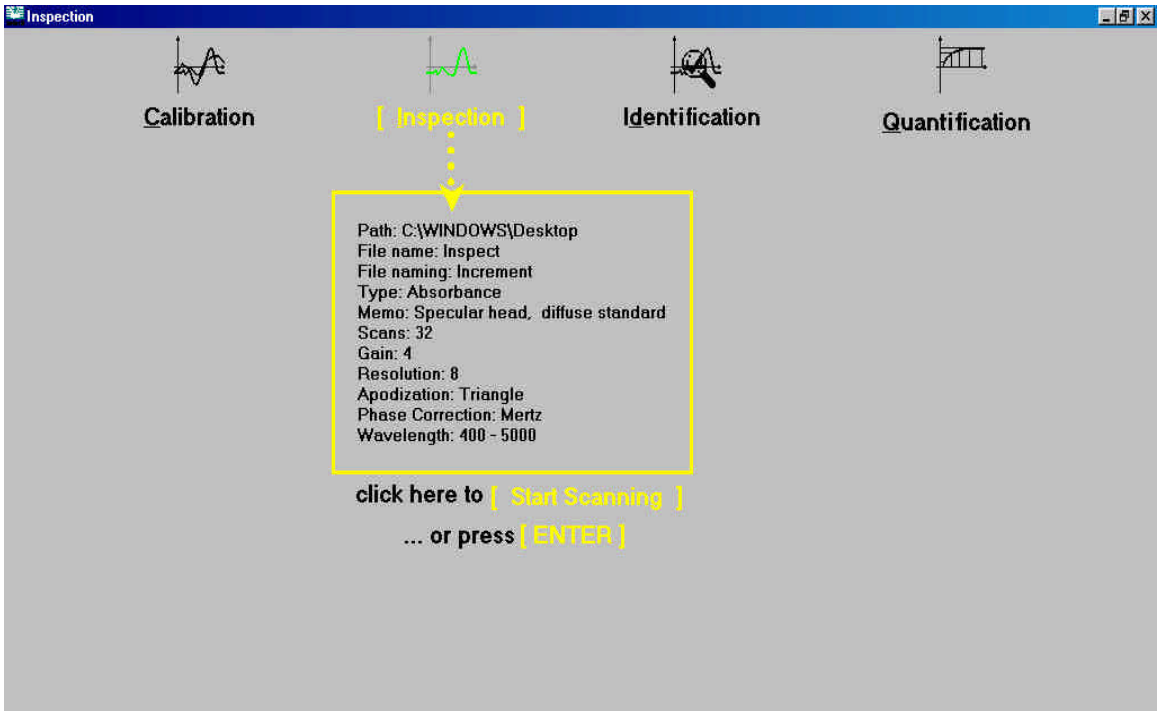

Figure 20. The Inspection Screen is designed for everyday surface inspections use by non-technical personnel.

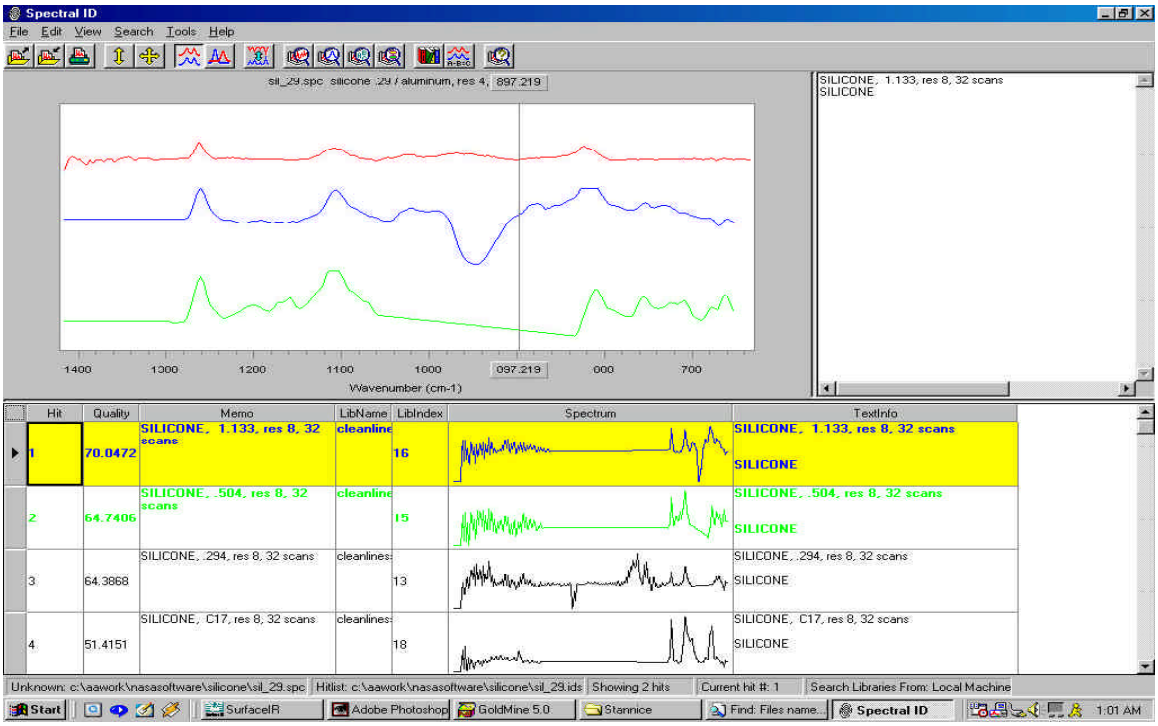

Figure 21.Identification of contamination is based on a search of spectral libraries in the computer. Libraries can be created by the operator using known contaminants on calibrated coupons.

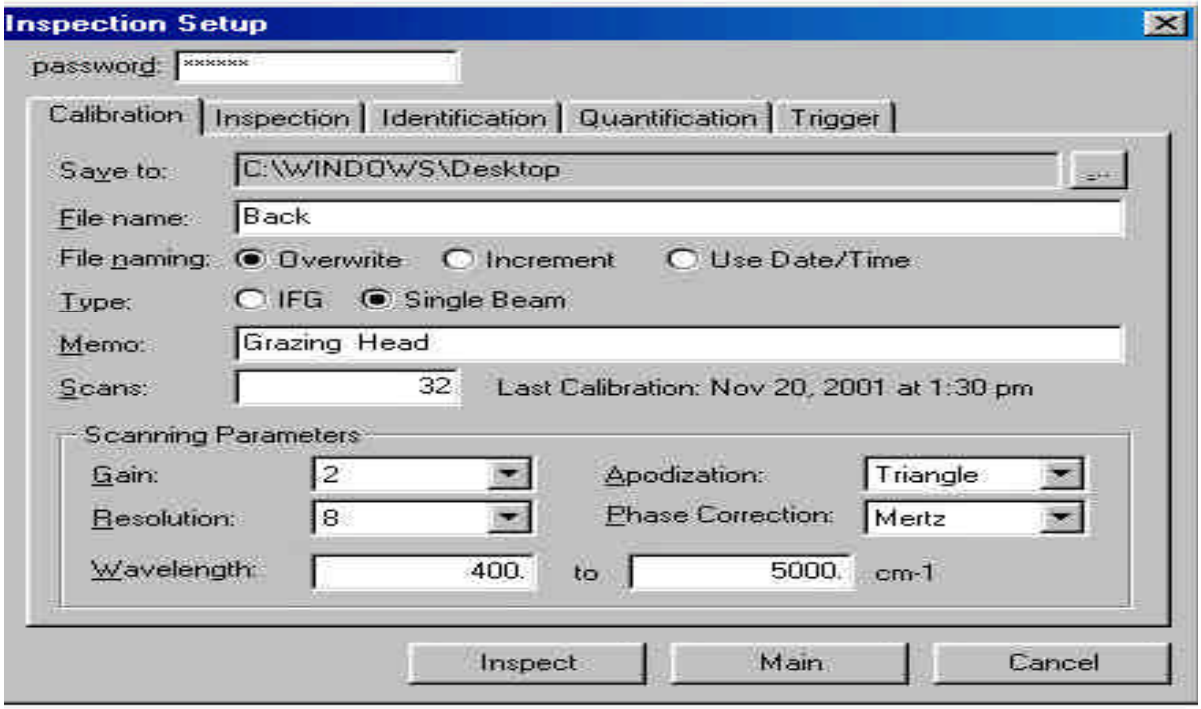

Figure 22. Operator selects parameters for routine operations of calibration, inspection, identification, and quantification.

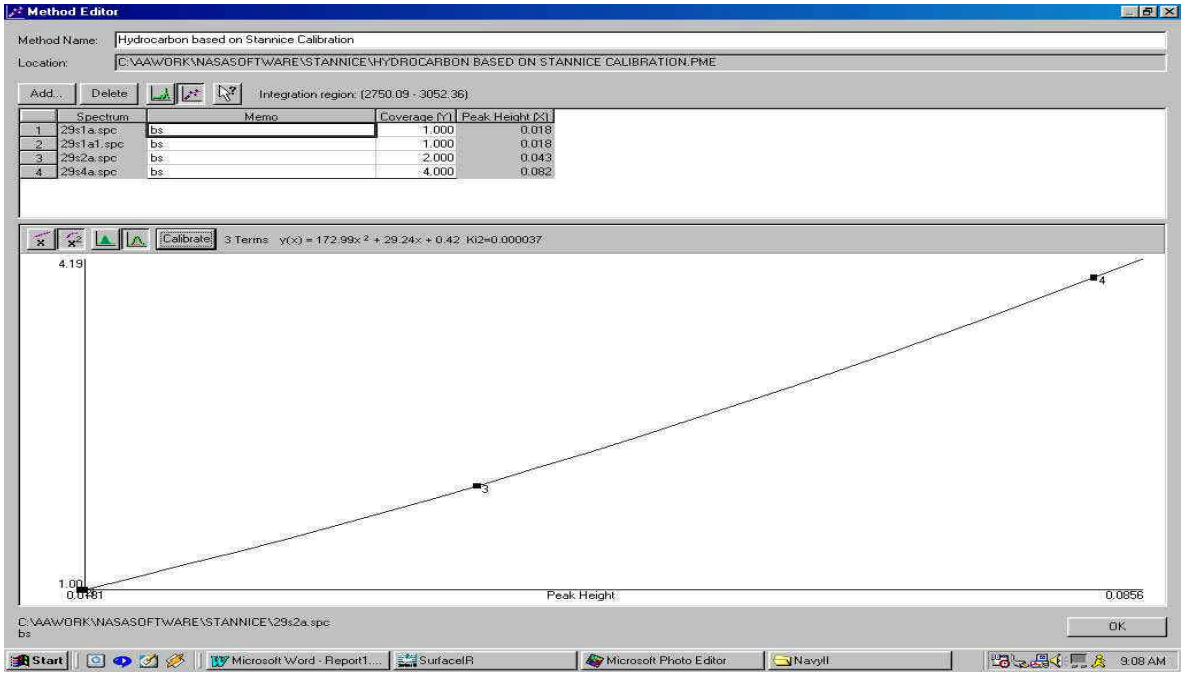

Figure 23. Quantitative analysis is accomplished by generating calibration curves from calibration coupon spectral data.

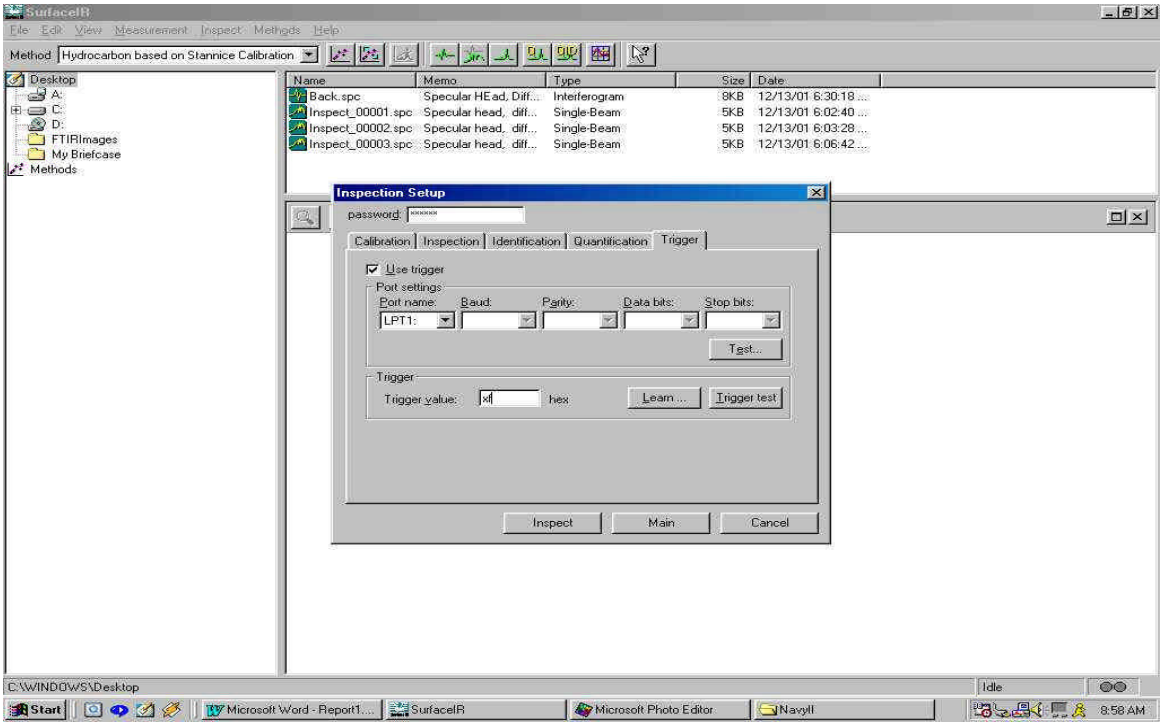

Figure 24. The remote trigger can be set up at the computer.

D. Laboratory Specimens Analyzed by Portable FTIR Device

During Year 2, additional test coupons of contaminants A through D were prepared in the NFESC laboratory and analyzed on both the commercially available laboratory device and the portable instrument. Figures 25, 26, 27, and 28 show comparative spectra of Contaminants A through D on 80-grit (roughest test surface) Aluminum 7075 panels. Both instruments used polarizers and both collected spectra at a 75-degree grazing-angle of incidence.

The SOC instrument consistently outperformed the laboratory device in terms of signal-to-noise ratios. In the spectra presented in Figures 25, 26, 27, and 28, the noise level differences are visually dramatic. The lower noise levels allow the FTIR operator (and software) to more easily and accurately assess the contaminant's identity and quantity on the surface of the coupons. The patented design of the SOC FTIR optics allows for this improvement.

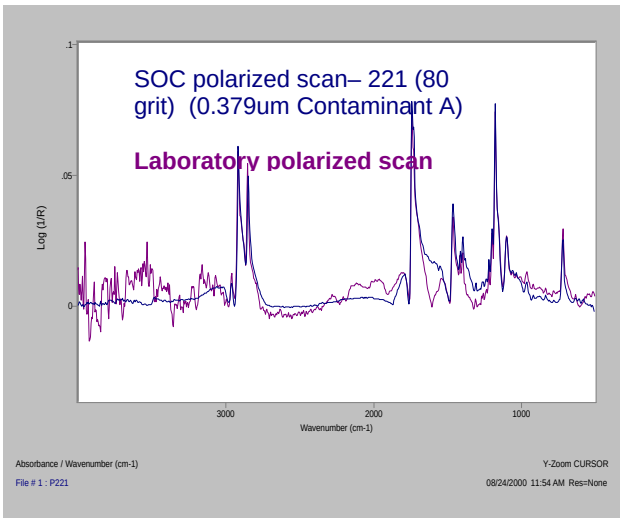

Figure 25. Contaminant A.

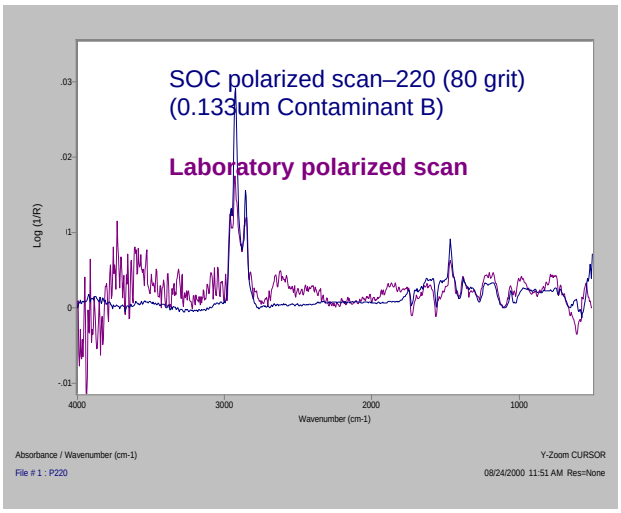

Figure 26. Contaminant B.

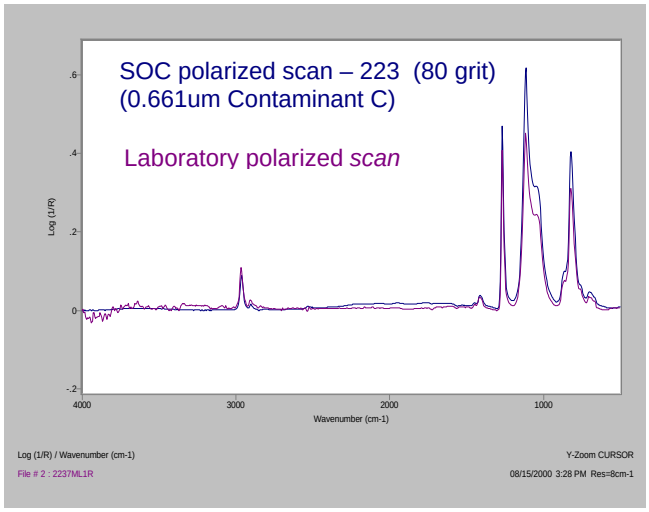

Figure 27. Contaminant C.

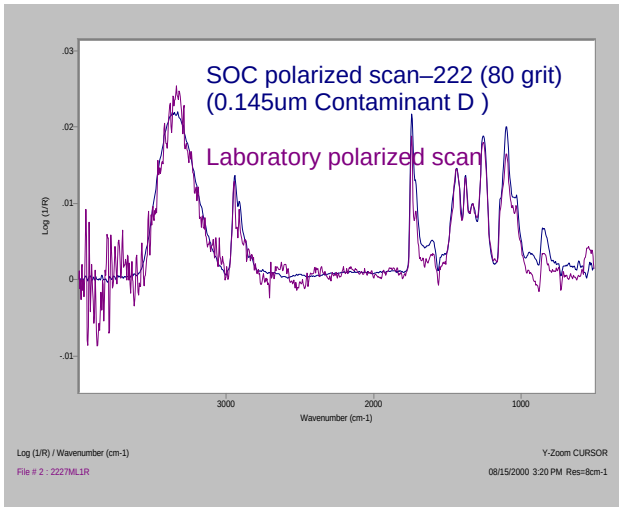

Figure 28. Contaminant D.

E. Real-World Specimen Analysis - Comparison of Laboratory and Portable Devices

Selected materials received from the North Island Naval Aviation Depot (NADEP), San Diego CA, and Hill Air Force Base Depot, Ogden, UT were analyzed by both the laboratory and portable grazing-angle devices. North Island samples included a contaminant mixture, or "soil" mix, specially prepared to represent four common products used in aircraft maintenance and repair activities and which pose contamination problems to surrounding parts. The substrates included aluminum panels with various surface treatments typically used in aircraft parts, i.e., etched and deoxidized, dichromate conversion coated, and Type II sulfuric acid anodized.

Hill AFB also provided NFESC with a series of aluminum aircraft panels. The panels were chromic acid anodized and alodyned (dichromate conversion coated) Aluminum 7075 in three stages of a stripping and cleaning process: Shop-cleaned with solvent and rags, painted then plastic bead blasted to remove the paint, and a painted panel. Plastic blasting media is used on aluminum skin vice the harder silica containing media to prevent distortion and damage to the surfaces. Hill personnel were interested in detection of plastic blast media residue left on the surface of the panels. This residue is often invisible to the naked eye and is suspected of causing adhesion problems in subsequent coating applications.

NFESC analyzed all of the test panels with its variable-angle laboratory reflectance unit before providing them to SOC. As with the specimens prepared on commercial coupons, for a given number of scans and background material, the prototype device consistently produced spectra with better signal-to-noise levels than those produced with the laboratory unit. Overall, intensities for peaks of a given contaminant and coupon were the same for both the SOC FTIR prototype and the laboratory unit. Figures 29, 30, 31, and 32 show comparative spectra of North Island soil mix on aluminum panels with the various surface treatments.

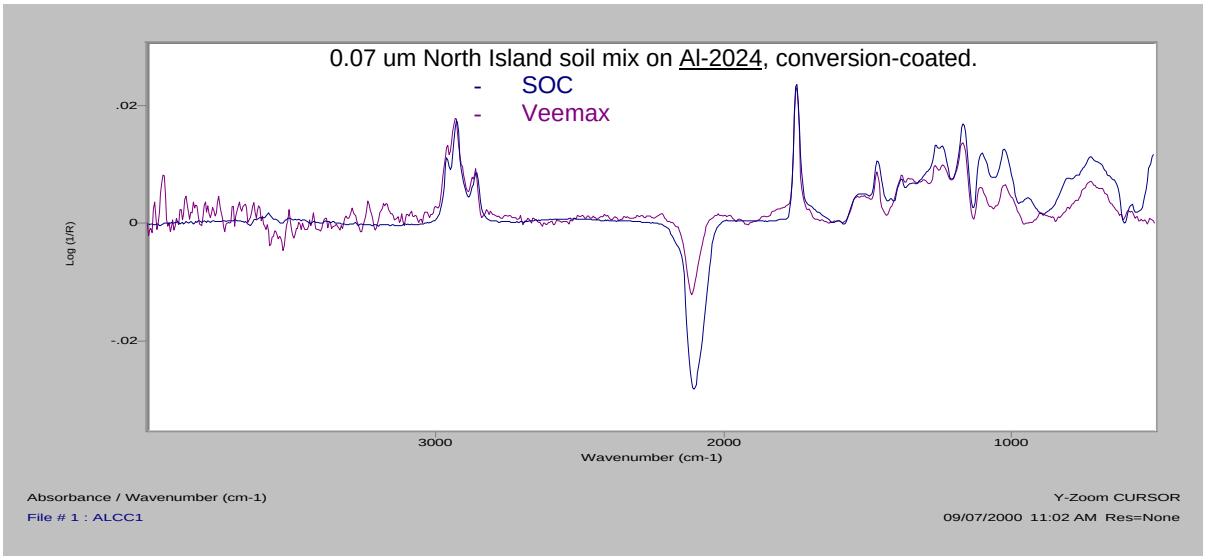

Figure 29. North Island soil mix on conversion coated aluminum. SOC versus laboratory grazing-angle FTIR devices.

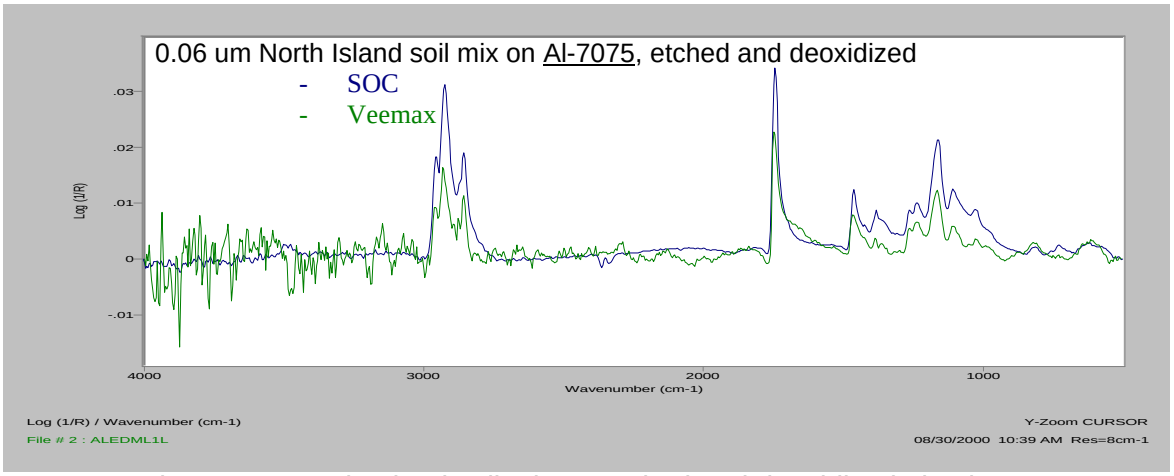

Figure 30. North Island soil mix on etched and deoxidized aluminum. SOC versus laboratory grazing-angle FTIR devices.

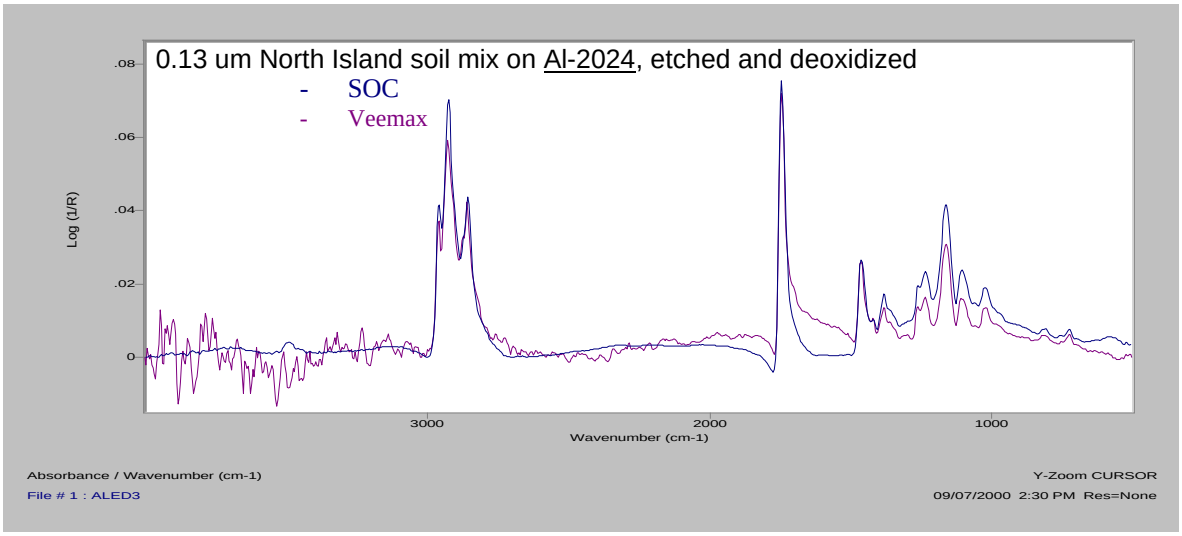

Figure 31. North Island soil mix on etched and deoxidized aluminum 2024. SOC versus laboratory grazing-angle devices.

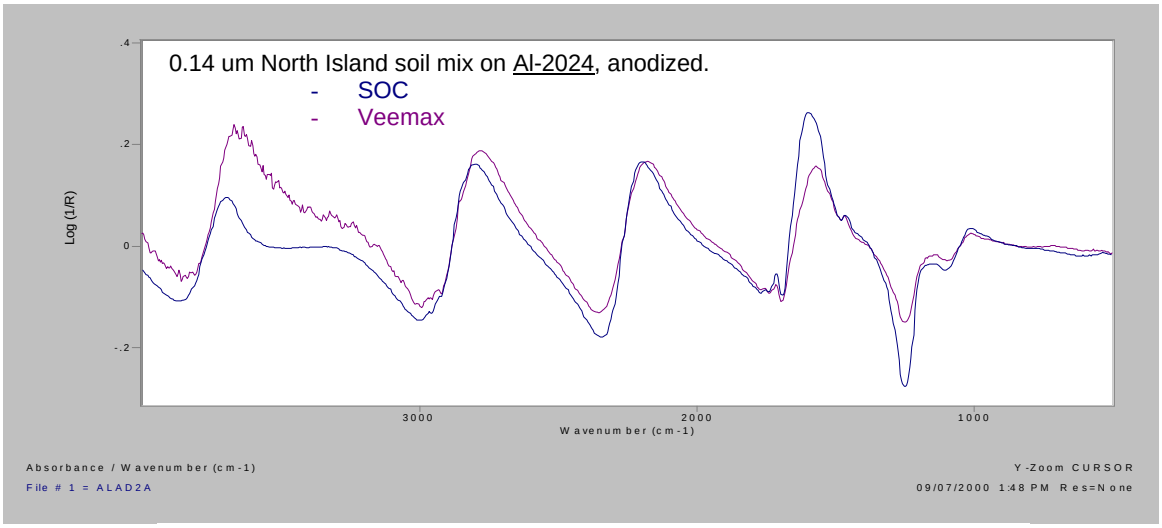

Figure 32. North Island soil mix on aluminum coated with a typical aircraft paint.

Representative noise levels of the portable device were calculated using an Al-7075 etched and deoxidized coupon and the "SOC 400 Noise Analyzer" software, installed in the FTIR prototype. A polynomial was fitted to the curve and the peak-to-peak value was calculated for the specified region. Values of 0.00031 log[1/R] (absorbance) units with sigma (s) = 0.0000674 were obtained. These noise level calculations provide the user with a method for determining minimum detection limits, as well as serving as a diagnostic on the general "health" of the instrument. From this data, and data obtained on earlier laboratory specimens, the FTIR device is estimated to have a detection level of approximately 0.22 µg/cm^2 for hydrocarbon contaminants.

Note the strong sinusoidal pattern obliterating any contaminant peaks in the spectra of the Type II sulfuric acid anodized panels (Figure 32). The sinusoidal interference is produced by multiple interfering reflections of the grazing-angle IR beam within the anodized aluminum oxide layer. As the thickness of the layer varies microscopically across the surface, the period of the sine wave is also changed. This makes it very difficult to "cancel out" the interference using a reference with the same anodized surface. If the thickness of the anodized films do not exactly match, dividing the sample spectra by a background reference of a clean anodized panel will just produce a third sine wave.

Different combinations of background and samples substrates were used with the laboratory device to investigate the feasibility of canceling out the interference. At a 75-degree angle of incidence, attempts to obtain readable contaminant spectra were unsuccessful. However, when the angle of incidence was lowered below the grazing-angle range, a spectrum with visible contaminant peaks was obtained. This demonstrated that grazing-angle reflectance FTIR is NOT well-suited to analyzing contaminants on specimens with optically thick substrate treatments such as Type II sulfuric acid anodization.

An attempt was also made to correct the sinusoidal spectra electronically by using the "ZAP" function in the FTIR operating software. This function allows an FTIR operator to remove interference "fringes" visible in the interferograms, the raw signal data, before

conversion to reflectance spectra. This was not successful. The fringes due to the sinusoidal wave were not distinguishable in the interferogram signal.

Since they were optically thin, the other substrate treatments were successfully analyzed by the grazing-angle devices. Figure 33 below shows the SOC data and calibration curves for two types of aluminum (2024 and 7075) and two types of metal treatment (etched & deoxidized, and dichromate conversion coated) soiled with the NADEP North Island mixture. Overall, very good linearity is observed for the four different substrates.

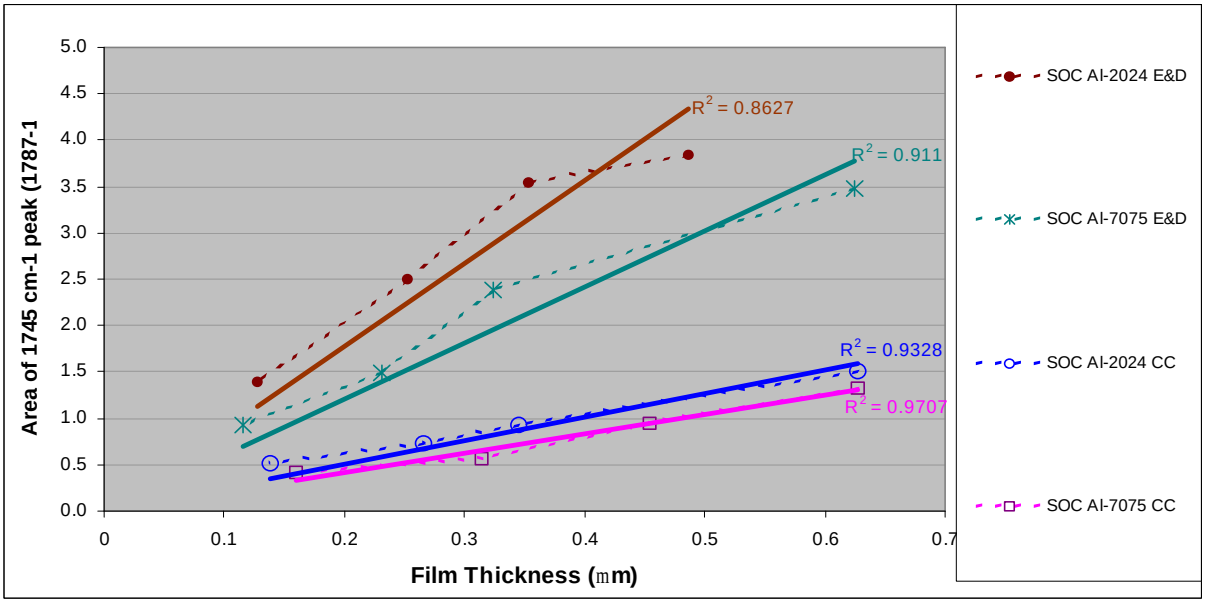

Figure 33. Calibration curves for North Island soil mix on etched and deoxidized, and dichromate conversion coated aluminum (series 2024 and 7075).

The spectra of the Hill AFB samples obtained on NFESC's laboratory device are presented in Figures 34, 35, 36, and 37. In addition to the stripped specimens, a painted panel was analyzed as well. As anticipated, the grazing-angle device did not perform well for this optically thick specimen. The anodized panels, however, were successfully analyzed. This anodization on the panels from Hill AFB was a chromic acid anodization instead of the Type II sulfuric acid used at North Island. This treatment results in a much thinner surface layer, precluding the optical problems seen with the sulfuric acid anodization, and produces a more readable grazing-angle spectrum.

Figure 34 shows two anodized panels, painted then blasted. There is evidence of hydrocarbon contamination (peaks in circle) on both panels. The small but distinctive peak in the blue spectrum at approximately 1740 cm^{-1} (arrow) suggests some of the hydrocarbon contamination is due to an ester material such as that found in the plastic blast media used to strip the surface. The FTIR computer software allows the operator to zoom in on and enlarge peaks of interest for a more accurate assessment.

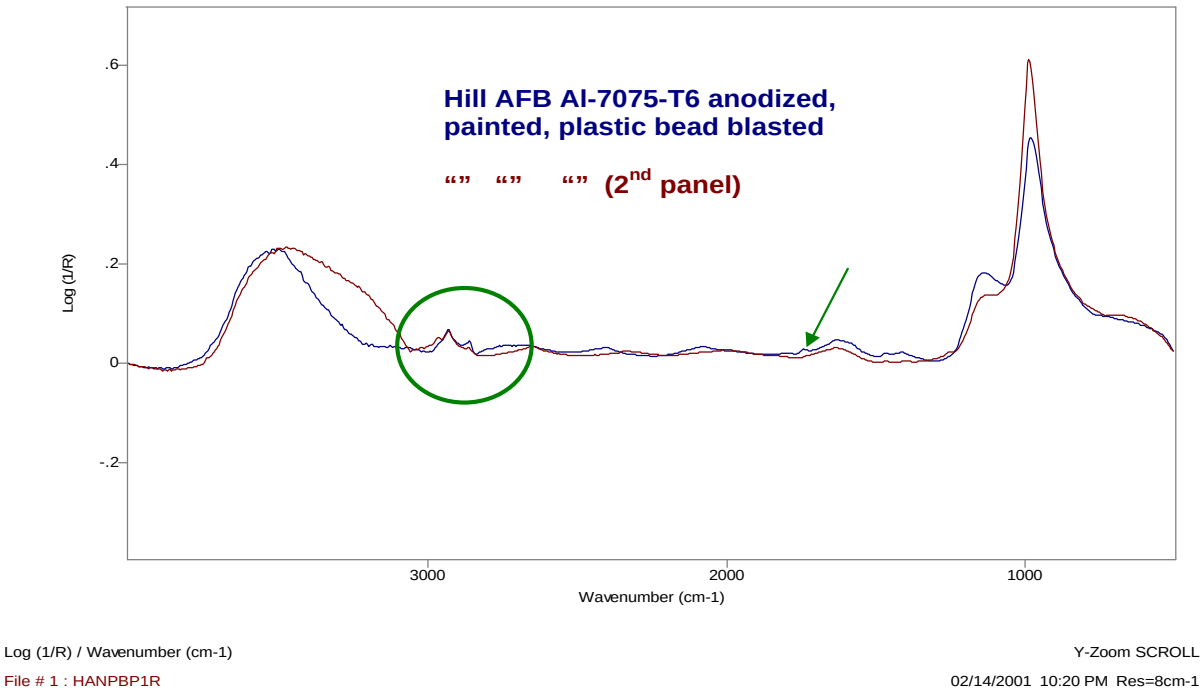

Figure 34. Two chromic acid anodized panels, painted then stripped with plastic blast media.

In Figure 35, the blue spectrum represents an alodyned, painted, then stripped panel. The blue spectrum displays strong peaks (circled) indicating a significant amount of an aliphatic hydrocarbon-carbonyl contamination. This spectrum is indicative of an acrylate, such as would be found in plastic blast beads. The brown spectrum, shown for comparison, is shop-cleaned and alodyned but not painted or stripped. The brown peaks are due to the alodyne finish, not hydrocarbon contamination.

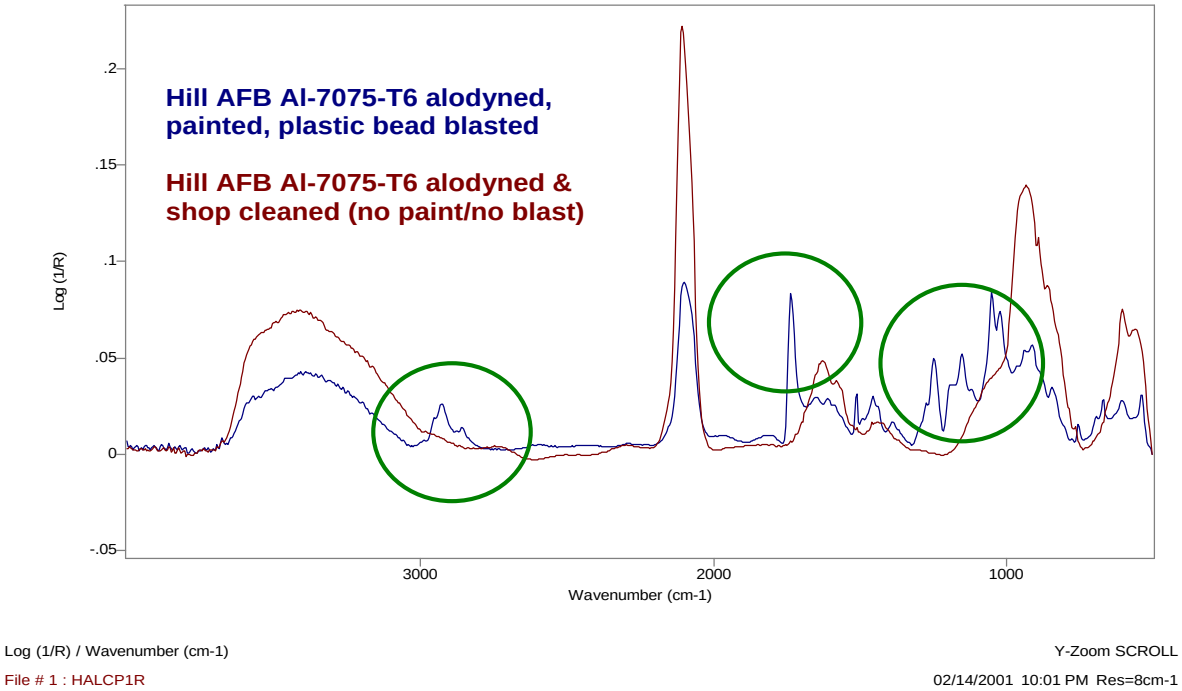

Figure 35. Alodyned panels representing two different processing conditions.

Figure 36 reveals inconsistent cleanliness levels on two aircraft panels cleaned manually with rags and solvent. There is evidence of hydrocarbon contamination (blue peaks in the green circle) on the anodized panel (shop cleaned). The alodyned panel (shop cleaned) appears to be clean (brown peaks are from alodyne surface, not hydrocarbon contamination).

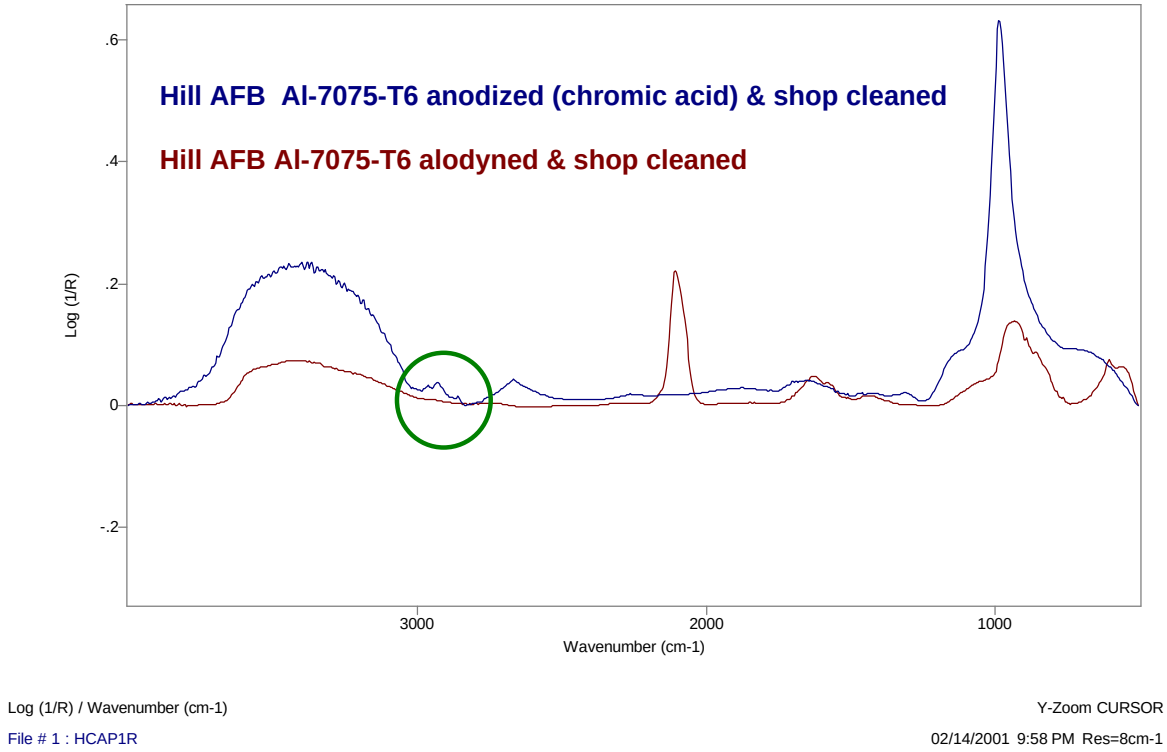

Figure 36. Two shop cleaned aircraft panels showing inconsistency in the manual cleaning technique.

Figure 37 shows a spectrum of a painted surface. No spectral detail can be seen due to the non-reflective nature of the surface and the increased absorption of the infrared beam by the optically thick organic paint layer. Other infrared methods (e.g., ATR, specular reflectance) are more appropriate for analysis of painted surfaces. An alternate specular reflectance optical head is available for use with the portable FTIR device. The specular reflectance head uses incident light at a much lower angle normal to the surface than grazing-angle techniques, making it better suited to the analysis of optically thick coatings and plastics.

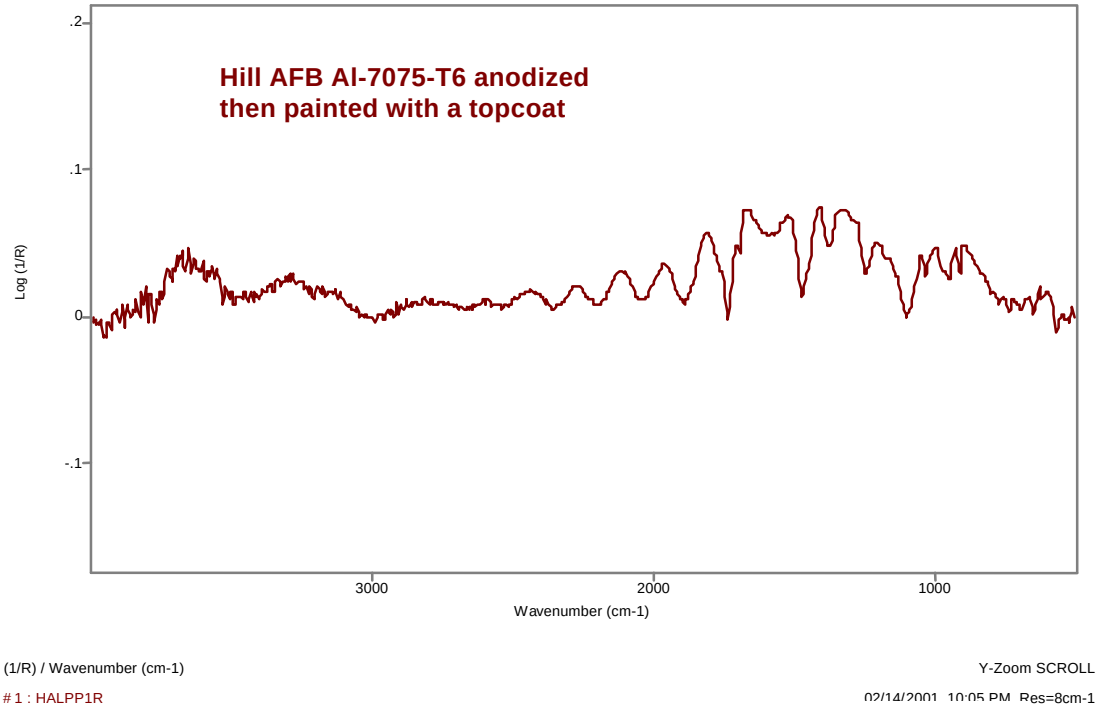

Figure 37. Grazing-angle spectrum of a painted aluminum panel.

In September 2001, the Boeing Corporation provided SOC with two series of stainless steel calibration coupons containing ultra-low levels of polystyrene and silicone contamination (lowest level was approximately 0.73 mg/ft^2 or 0.78 µg/cm^2). These coupons were prepared by NASA to be durable calibration standards with uniform thickness levels. SOC personnel analyzed the coupons on the grazing-angle FTIR device. Even at the lowest concentrations, which are near the detection limit of the instrument, the resulting spectra were clear enough to classify the materials. A linear progression was seen in the increasing intensity of the spectral peaks with increasing levels of contamination.

Figures 38 and 39 show spectra of the polystyrene-contaminated coupons at varying levels of thickness. The listing of the panel coupons in order of most contaminated (top of list) to least contaminated (bottom) corresponds proportionally to the spectra, i.e., the spectrum of the most concentrated panel has the strongest peaks. Figure 38 shows the entire spectral range. Figure 39 expands the area from 1600 to 600 cm^{-1}. The spectra exhibit excellent signal-to-noise levels given the minute levels of polystyrene contamination.

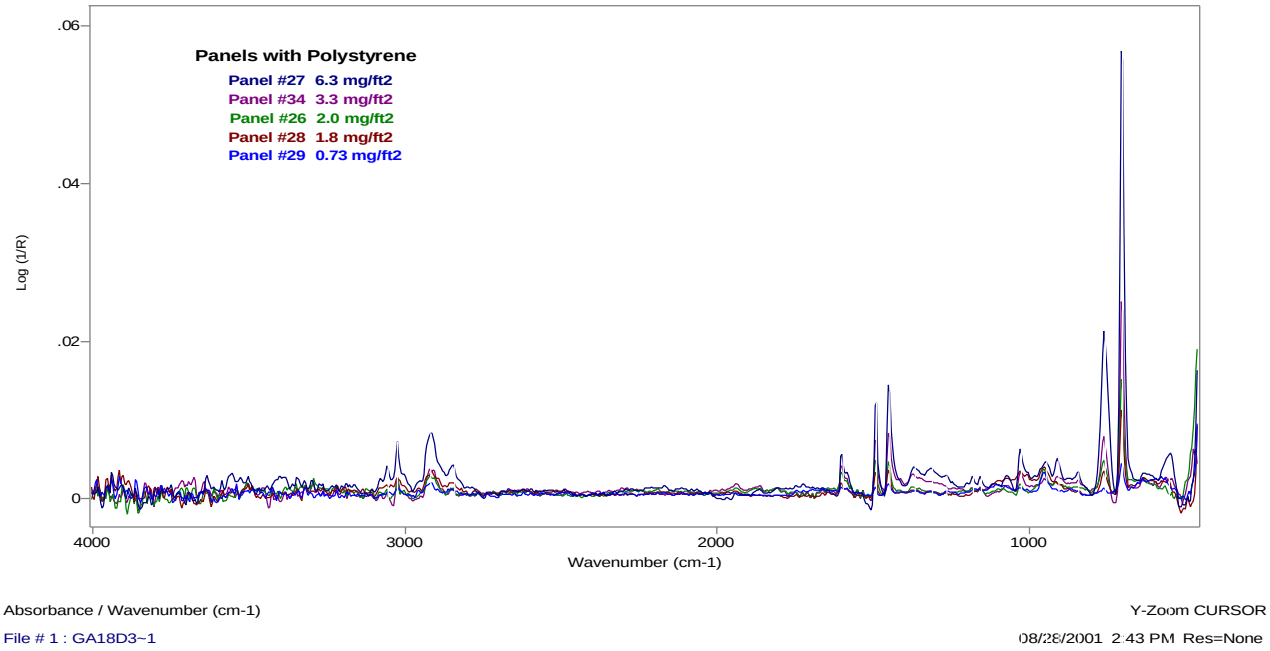

Figure 38. Spectra of varying levels of polystyrene on stainless steel panels.

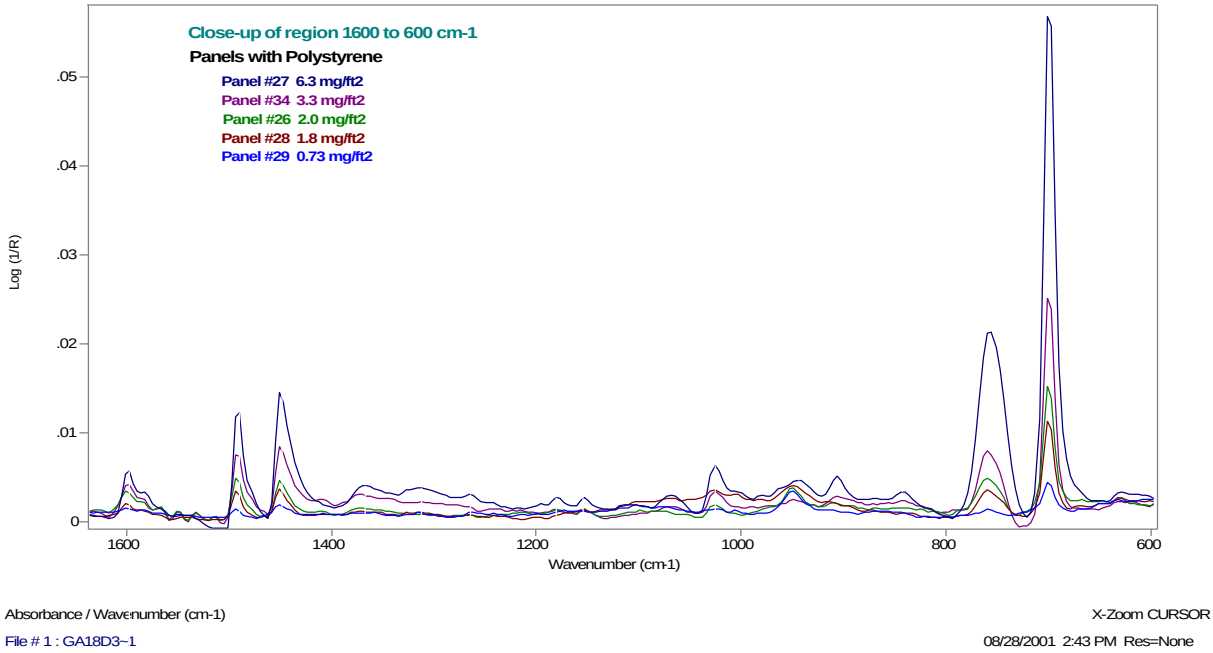

Figure 39. Close-up of lower wavenumber region.

F. Field Demonstrations of the Portable Grazing-Angle FTIR

Successful laboratory testing allowed NFESC and Sandia National Laboratories to perform an early field demonstration of the SOC portable FTIR device at NADEP North Island, San Diego CA, in December 2000.

NADEP North Island personnel reported cleanliness problems from leaking hydraulic fluid or fuel from the seams or connectors of the fuselage and wings. These fluids contaminate the aircraft skin, leading to subsequent coating application problems. Additionally, zero or low VOC coatings are being mandated by environmental emission regulations. The reduced amount of free solvent (used as a vehicle in paint formulae) is no longer able to displace or dissolve low levels of surface contamination and may lead to adhesion problems.

The unit was tested on a dichromate conversion-coated aluminum wing of an F/A-18A aircraft. The wings had been cleaned in preparation for coating. Photographs of the in-situ measurement using the FTIR unit are shown in Figures 40 and 41. The device detected the dichromate coating as well as a small amount of hydrocarbon contamination. Depot personnel did not expect that the wing surface would contain detectable contaminants. The device had the ability to monitor this low level of contamination invisible to the naked eye. Figure 42 shows the spectrum of this contamination, as well as the chromate conversion coating, represented by the much larger peaks at approximately 2100, 900, and 600 cm^{-1}. The FTIR was operated in an "unpurged" state and the fringed peak patterns evident above 3800 cm^{-1} and between 1700–1400 cm^{-1} are from water vapor trapped inside the FTIR compartment. The distinctive but inverted doublet peak at 2300 cm^{-1} is due to a higher concentration of trapped carbon dioxide in the FTIR during collection of the background spectrum than during collection of the sample spectrum. The water vapor and carbon dioxide, naturally present in air, can be easily removed by purging the FTIR with a portable cylinder of nitrogen or dry air. This removes the interfering absorbances and improves the quality of the spectrum.

Figure 40. Portable grazing-angle FTIR employed for cleanliness verification of an F/A-18A aircraft wing at North Island.

Figure 41. Close-up of the FTIR device sampling a wing awaiting final coating application after cleaning and conversion coating.

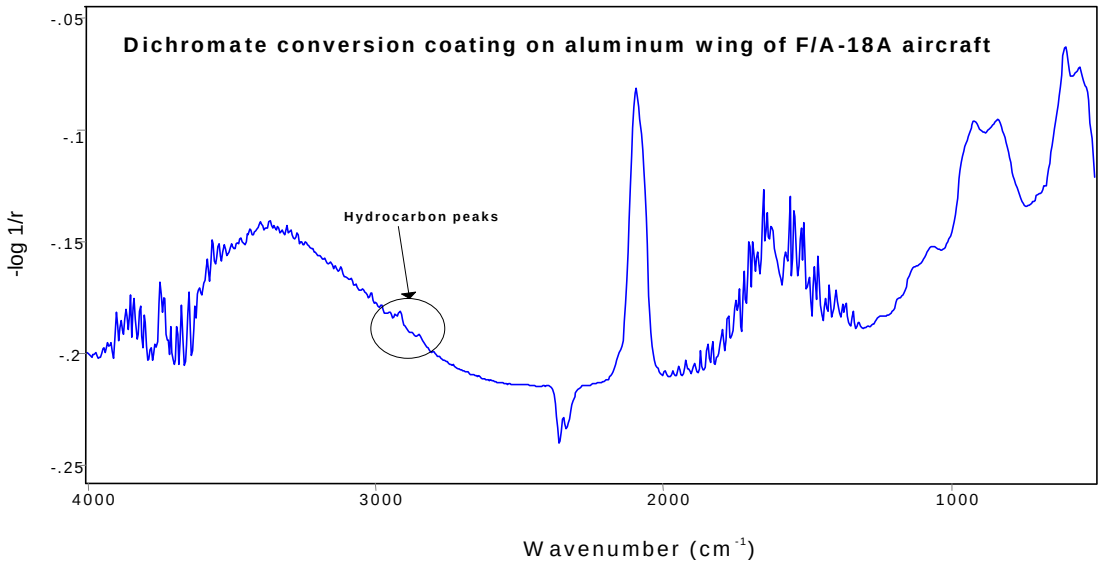

Figure 42. FTIR reflectance spectrum (unpurged) of F/A-18A aircraft wing showing presence of chromate conversion coating AND presence of hydrocarbon contamination.

North Island personnel were also interested in using the portable FTIR instrument to detect a trivalent chromium conversion coating on aluminum aircraft parts. This treatment process results in a very thin oxide coating on the metal surface that is invisible to the naked eye, unlike the more conventional dichromate conversion coating. Shop personnel were searching for a method to confirm that the coating had "taken" on the metal surface during the treatment process. The FTIR device was able to detect the coating on the surface of a test panel, providing confirmation that the coating was indeed on the surface (Figure 43). Clean, bare aluminum containing no treatment will give a flat baseline when analyzed. In addition, the relative thickness of the coating can be determined by the intensity of the spectral peaks.

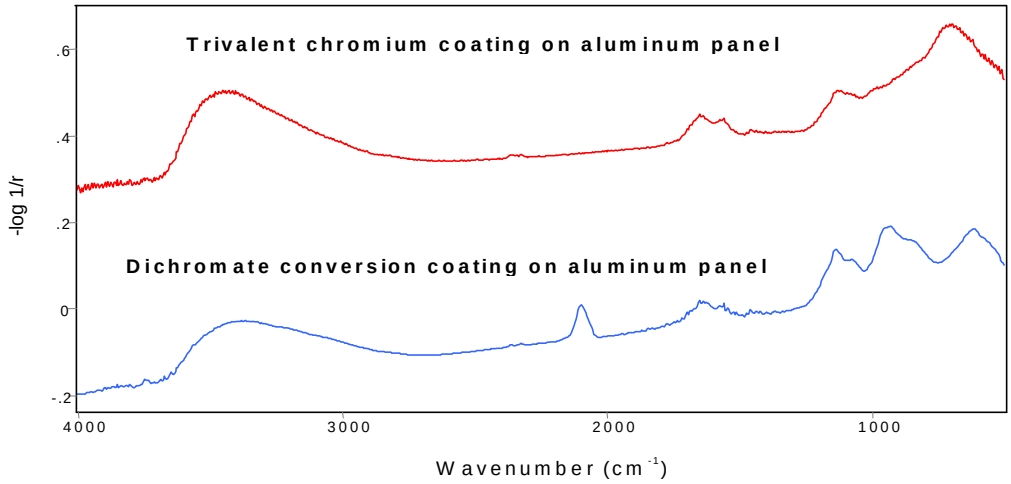

Figure 43. Comparison of grazing-angle spectra of a conventional chromate conversion coating and a trivalent chromium coating on aluminum panels.

Following the successful field-test at NADEP North Island in December 2000, a second demonstration of the FTIR prototype was conducted at Hill Air Force Base in Ogden, Utah in January 2001. number of Hill AFB maintenance personnel were in attendance, as well as representatives from NFESC, Sandia National Laboratories, and Surface Optics Corp.

The demonstration occurred in one of Hill's large hangar facilities on an A-10 aircraft. The aircraft had undergone cleaning of its aluminum skin, including stripping of an old coating using plastic blast media. The aircraft was sampled by the FTIR in three locations: (1) bare aluminum on a landing gear door, (2) bare aluminum on the underside of a wing, and(3) chromic acid anodized aluminum on the underside of the wing.

Figure 44 below shows samples of spectra collected. All spectra showed the presence of hydrocarbon and carbonyl contamination, indicating that the aircraft skin was contaminated. A prominent carbonyl band at 1735 cm^{-1} is suggestive of plastic bead blasting media used at Hill to remove old coatings. The anodized surface layer was also detected on the aircraft wing. This spectrum showed several very broad peaks due to the anodized layer. A large aluminum oxide peak was clearly visible at 930 cm^{-1} but did not mask the small but sharper hydrocarbon and carbonyl contamination peaks.

The portable instrument was able to detect the invisible contamination, as well as distinguish the anodized coating. In addition to waste stream reductions in cleaning and coating operations, Hill personnel indicated that paint failure analysis (i.e., looking for foreign material on the surfaces of aircraft that may have affected the previous coating's adhesion) is important due to the high cost of stripping and recoating each aircraft. Single aircraft may cost from the 10's to the 100's of thousands of dollars to strip and recoat.

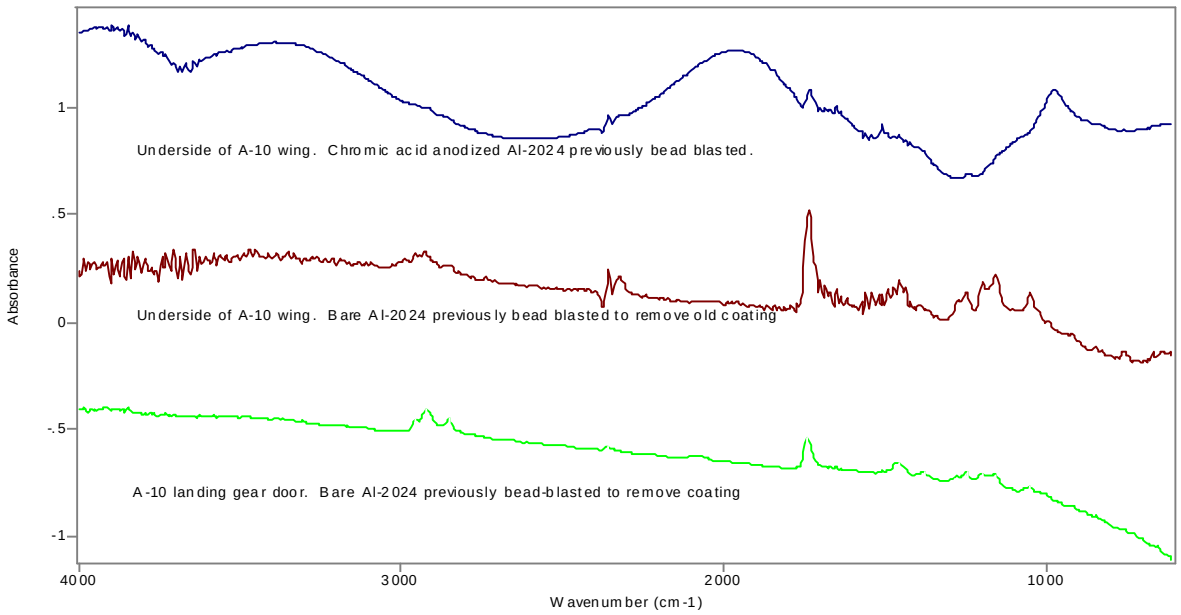

Figure 44. Spectra of aircraft surface contaminants and surface treatments on selected areas of an A10 aircraft at Hill AFB.

Figures 45, 46, 47, and 48 show the device at work sampling different areas on the aircraft.

Figure 45 . FTIR unit sampling a landing gear door. Laptop computer controller is in the foreground.

Figure 46. Close-up of FTIR device sampling the landing gear door surface.

Figure 47. Reorientation of FTIR device on the tripod to analyze the underside of a wing.

Figure 48. Operators observe collection of data by the FTIR and instantaneous conversion of data to a spectrum on the computer screen.

Also examined during the demonstration were a series of circular 300M steel landing gear parts. Several of the specimens had been "reverse etched" in chromic acid. While an etched surface is desirable for this application, exposing the material for too long a period in the etching solution causes silicon, a component of the steel alloy, to accumulate on the etched surface in the form of silicates. This adversely affects the part's performance and ability to be coated.

A non-etched, reflective part, and two etched parts were analyzed by the FTIR. The etching exposure times for the two etched parts were 2 minutes and 30 minutes, respectively. The FTIR was able to detect a considerable amount of hydrocarbon and carbonyl contamination on the surface of the non-etched part. It was unable to determine any surface components on either etched part, however. These etched surfaces were dull and considerably rough. Hill personnel indicated that the surfaces could be as rough as 700 micro-inches R_a. In contrast, the test coupons used in the laboratory extended to a surface roughness maximum of approximately 250 R_a.

The non-reflective, rough surfaces of the etched parts were not conducive to grazing-angle analysis. The FTIR technique known as DRIFTS or diffuse reflectance is better suited to analyzing rougher surface profiles. SOC analyzed a number of these parts back at its facility with their DRIFTS optical head installed in the portable FTIR. However, because of the extreme levels of roughness and the high amount of carbon in the steel, the diffuse reflectance technique also failed to provide readable spectra.

Feedback from the first and second demonstrations let to implementation of improvements to the prototype device and a third follow-up demonstration in March 2002 at Hill AFB. Figures 49, 50, 51, 52, 53, 54, 55, 56, and 57 show scenes of the demonstration in progress.

Two aircraft in the maintenance hangar were chosen for the FTIR demonstration: a C-130 and an F-16. The C-130 had been stripped to bare aluminum using plastic blast media Type V (polymethylmethacrylate). The F-16 had been stripped, also using Type V plastic blast media, to its chromic-acid anodized aluminum surface with yellow epoxy primer still present in some areas.

NFESC prepared two series of calibration coupons for the demonstration. All coupons were Aluminum 7075. Three different finishes were selected. A third of the coupons were bare aluminum, another third were chromic-acid anodized aluminum, while the remaining third were dichromate-conversion coated (alodyned). The coupons were further separated in two groups to receive one of two contaminants: plastic blast media Type V or the North Island hydrocarbon mixture. SOC analyzed the coupons on the portable FTIR, and created calibration curves for use during the demonstration.

The main cleanliness problem reported by Hill personnel for these aircraft was the retention of plastic blast media residue on the surfaces of the aluminum skin. This residue, if present in sufficient concentration, is detrimental to future coating operations. The FTIR device was easily able to detect this residue on the C-130, even though the calibration data suggested that its level was < 18 $\mu g/cm^2$. Personnel present concurred that the upgrades to the software made the unit more user friendly. The new software uses one-click icons and windows to direct the operator to prepare a calibration curve, analyze an area on the aircraft, and compare that contaminated area to both the calibration curve (to quantify the contaminant), as well as to a library of contaminants (to classify or identify the contaminant).

The calibration coupons prepared at NFESC contained relatively high levels of contamination, i.e., the accuracy of the calibration at the bottom of the curve (< 10 $\mu g/cm^2$ contamination) was questionable. This caused a problem with one of the analyses. A negative concentration value was calculated by the computer for an unknown contaminant on the aircraft

surface, based on this calibration curve. The noise in the baseline of the unknown spectrum, compounded with the problem of accuracy at the low end of the calibration curve, caused this difficulty. The solution to this problem is to obtain calibration coupons that represent a much lower range of contaminant concentration, such as those described earlier and prepared by NASA. Such coupons are more difficult to prepare and require more sophisticated techniques. NFESC coupons were prepared by a crude brush application technique. NFESC does not have the capability to produce the ultra thin uniform films. However, a number of commercial sources are available to provide this service. Once prepared, and with careful handling, calibration coupons containing the polymethylmethacrylate contaminant can be used over and over. NASA was able to prepare coupons with very low concentrations of silicone and polystyrene contaminants for Boeing Corporation. These coupons were used multiple times over the course of several months.

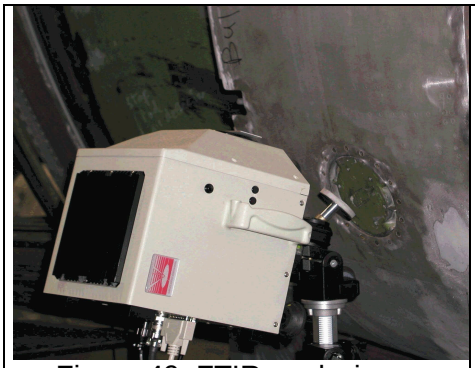

Figure 49. FTIR analyzing a calibration coupon near the C-130.

Figure 50. FTIR analyzing C-130 bare aluminum belly.

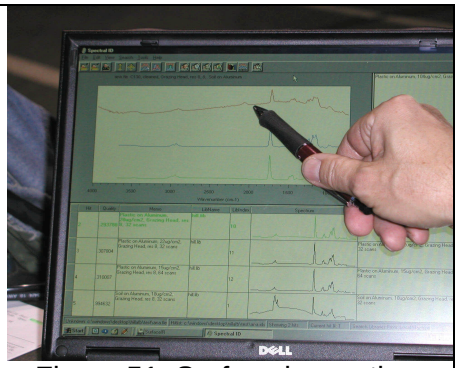

Figure 51. Surface inspection software performing a library search on a contaminant.

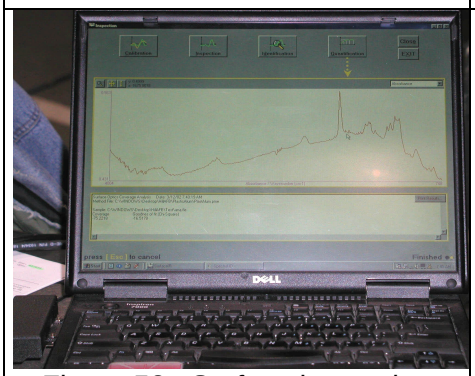

Figure 52. Surface inspection software on laptop computer showing a spectrum of the C-130 surface.

Figure 53. FTIR operator at the C-130 demonstrating hand-held FTIR operation.

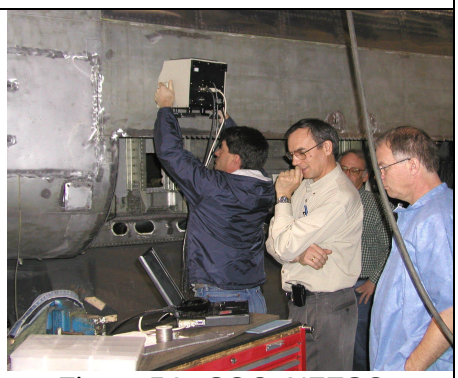

Figure 54. SOC, NFESC, Sandia, and Hill personnel analyzing the C-130 surface.

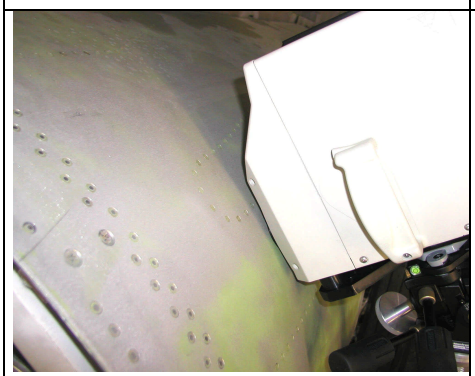

Figure 55. Close-up of the FTIR analyzing an F-16 landing gear door.

Figure 56. FTIR analyzing an area containing yellow epoxy primer.

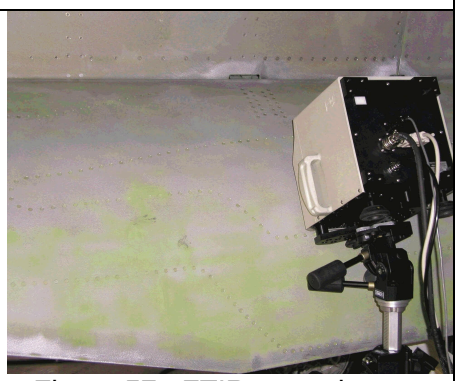

Figure 57. FTIR operating on a camera tripod to analyze the F-16.

Less successful was the analysis of the F-16, due to the presence of the epoxy primer. Since the epoxy primer is organic, its IR absorbance peaks interfere with those of the plastic blast media. This makes it difficult or impossible to determine the presence or absence of the blast media residue. A more successful analysis of the F-16 could be accomplished if a separate sample of the epoxy material could be obtained and analyzed. If the plastic blast media and the epoxy show any significantly different absorbance peaks in their spectra, that spectral region could be used to discern the presence of the plastic media regardless of the presence of any epoxy. Also if the thickness of the epoxy primer were to be determined using a calibration curve of known amounts of epoxy, the spectral features could be subtracted out by the FTIR computer, leaving a spectrum of just the plastic blast media.

In May 2001 at the CleanTech International Cleaning Technology Exposition in Chicago IL, the grazing-angle FTIR device received the "2001 Outstanding Technology in Critical Cleaning" Award (Figure 58). This award is presented annually by the vote of subscribers to CleanTech Magazine, a monthly publication that reports on cleaning issues important to advanced technology and industrial applications (including aerospace and military).

Figure 58. Surface Optics Corp, represented by Dr. Martin Szczesniak, with the 2001 CleanTech Award plaque.

G. Economic Cost Analysis for the Portable Grazing-Angle FTIR

A cost analysis for the FTIR prototype was performed for the FTIR grazing-angle spectrometer system using a real-life application. The analysis was performed using ECONPACK 2.1 software, a DOD economic analysis package developed by the Army Corps of Engineers. The application considered was the refurbishment of aircraft wing panels at NADEP North Island. It was proposed that NADEP North Island may process on the order of 30 wing panels per year, depending on operational mission status, of which approximately 10 could be "infant mortality" coating failures due to improper surface preparation.

NADEP North Island personnel provided input on cost data to perform stripping, cleaning, and recoating tasks. Additional input on labor rates and material costs was provided by members of the SERDP Pollution Prevention review panel and the project's Technical Advisory Committee (which included NADEP North Island personnel). The purchase cost of the FTIR instrument is approximately $60K and was also factored into the analysis.

Because of its high sensitivity in detecting hydrocarbon contaminants, it was estimated that the FTIR would be able to catch 50% or more of contaminated wings missed by visual inspection. This would be translated into a 50% reduction of the number of wings seen for refurbishment at the depot in out-years, assuming the cause of the infant mortality was surface contamination. Over the life of the FTIR instrument, the number of wings seen back at the depot for this refurbishment should continually decrease. However, to simplify the analysis, it was assumed that a 50% reduction of the original number of wings would occur each year after the first year, during which no reduction would occur.

With all of the provided input, an economic analysis was performed and a Net Present Value (NPV) was calculated for both the current inspection method, visual examination and water break testing, and the new inspection method using the grazing-angle device over an estimated service life of 8 years. Figure 59 shows the results as a function of NPV. The discounted payback period for the FTIR is 4 years, after which the FTIR becomes economically favorable for this application.

The analysis indicates the first 4 years would be unfavorable, due to the high purchase price of the FTIR. Figure 59 presents an analysis for only a single application at a given depot, with the entire burden of the FTIR's purchase price and service cost being supported by this single application. Additional savings from multiple applications of the instrument would greatly improve the FTIR's economic viability and substantially reduce its payback period.

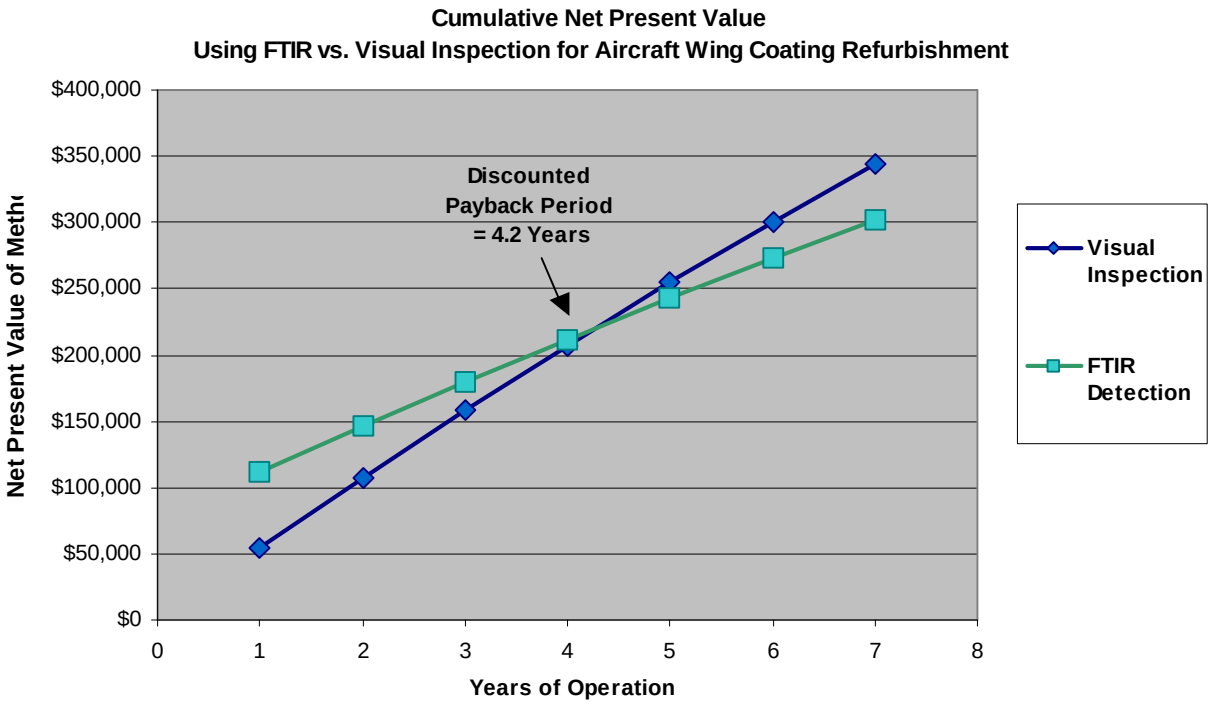

Figure 59. Net Present Values for using FTIR versus visual inspection for aircraft wing coating refurbishment.

To determine the reasonableness of a 50% expected reduction in refurbishments, a sensitivity analysis was performed in order to determine the effect of altering various cost elements on the NPV for both alternatives. It was determined that labor, by far, was the most sensitive cost factor in the economic analysis. The break-even point of the analysis was achieved by reducing overall labor costs (i.e., fewer wings) for stripping, cleaning and recoating by 26% when using the FTIR monitor inspection method. Figure 60 presents the results and input of the sensitivity analysis.

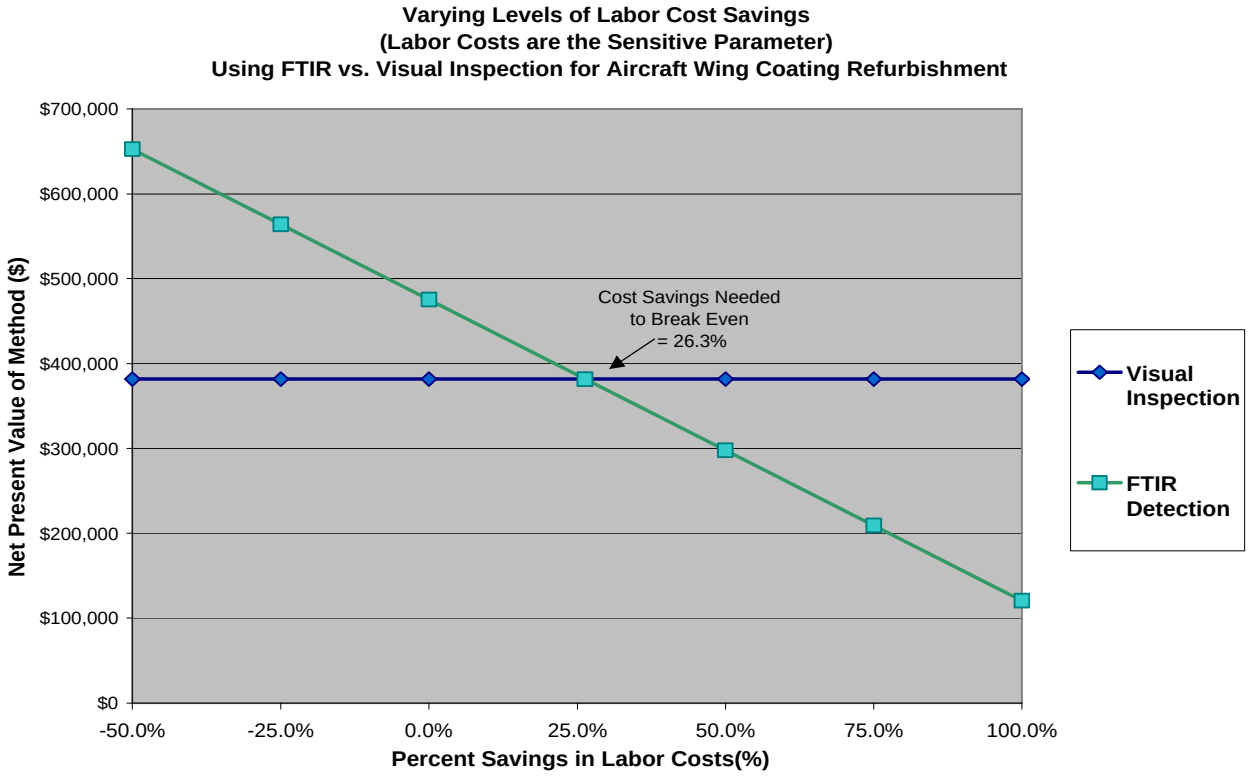

FTIR Sensitivity Analysis Information

Initialization:

- Assumption made that using FTIR may save nothing, i.e. 0% saving starting point.
- Analysis over service life of FTIR (~8 yr).

FTIR Procurement and Maintenance Contract

- This single refurbishment application bears 100% of the acquisition and maintenance contract costs for the FTIR.

Results:

- Sensitive parameter = LABOR for stripping cleaning and coating operations.
- Materials costs were NOT a sensitive parameter (i.e. changing the costs had little effect on the net present value).
- FTIR method must achieve approximately 26% reduction in labor costs to be competitive with the visual inspection method – for this application only.

Figure 60. Sensitivity Analysis of cost elements in the economic analysis of the FTIR for a wing refurbishment application.

Results of laboratory testing and preliminary field demonstrations show that the application of the FTIR could reduce or eliminate these premature coating failures. A uniform application of the technique with appropriate quality control procedures should improve the reliability of routine wing panel refurbishment, thus lengthening average lifetime and reducing associated labor costs for future maintenance. In addition to reducing labor costs associated with wing panel refurbishment, application of the infrared monitoring method will also reduce a proportionate amount of solvents and paint contaminated wastes currently generated in cleaning and recoating procedures.

5. DISCUSSION AND CONCLUSIONS

The laboratory and field tests performed during this project have demonstrated that the portable grazing-angle reflectance FTIR device is a useful, valuable method for cleanliness verification of many types of contaminants on reflective surfaces. Excellent sensitivity to low levels of contaminants is observed in both laboratory and field-testing environments for a variety of contaminants on aluminum, titanium, steel alloy, and stainless steel metals used in assemblies of DOD aircraft, weapons, and other components. The instrument is capable of promoting pollution prevention by limiting the generation of waste streams through refinement and careful monitoring of the cleaning process based on feedback from the device. It also has great potential to reduce or eliminate premature failures of surface coatings caused by a lack of surface cleanliness.

During Year 1 of the project, a series of test panels with well-characterized substrates, surface roughness levels, and contaminants were measured on a commercially available grazing-angle sampling device inside the laboratory. This testing successfully demonstrated the feasibility of the grazing-angle technique for cleaning verification.

During Year 2, further calibrated test panels were prepared with additional contaminants. A series of aluminum panels used for aircraft surfaces were also obtained from both a Navy and an Air Force depot to demonstrate, in the laboratory, the feasibility of the technique on real DOD hardware. A portable grazing-angle FTIR prototype was constructed and tested in the laboratory using the prepared test coupons and DOD supplied panels. A successful field demonstration of the portable device was conducted in December 2000.

During Year 3, the final year of the project, the FTIR device was field tested at an additional DOD depot. Based on feedback from that and the first field demonstration, the unit was improved with several upgrades to make it easier to use by non-technical personnel. The upgraded version was then field tested again at the second site. It was also tested with samples from the non-DOD sector, specifically ultra-thin films prepared on stainless steel by NASA for the Boeing Corporation. A cost analysis was performed on the use of the FTIR device for a particular cleaning and recoating process.

The following observations and conclusions are presented below:

a. Non-metallic or non-reflective surfaces are NOT well-suited to grazing-angle reflectance analysis.

Non-metallic composite materials are used in a variety of DOD components. Examples include the outer skins of the E and F series of F/A-18 jets, and the F-22. These aircraft contain outer skins made from graphite epoxy composites. North Island personnel described a problem experienced with these materials due to heat damage during aircraft operation. The damage is not visually detectable but a chemical change does occur which could affect the performance of the material. The current detection practice is to obtain plugs of the composite material and send them to a laboratory for TMA (thermal mechanical analysis). Successive laminated layers of the material are tested and the changes in Tg (the glass transition temperature) are tracked. This is an extremely time-consuming and costly process. The North Island personnel were seeking a better detection method, in particular a rapid on-site method.

However, as discussed in NFESC TM-2335-SHR, the reflectivity of non-metals varies widely. Non-metallic substrates that contain organic content will absorb infrared radiation and these absorptions are mixed into the resulting spectrum of the contaminant film. This reduces the overall energy that reaches the FTIR detector and complicates interpretation of the spectra. The p-component of incident radiation is not as greatly enhanced for non-metals as it is with metals (Ref 9). Also, the optimal angle of incidence varies with the substrate type for non-metals and may be below 60 degrees, the grazing-angle threshold.

Representative non-metallic composite materials were evaluated at NFESC. The grazing-angle technique was unable to distinguish the thin film of hydrocarbon contamination applied to the composites' surfaces. Additionally, as demonstrated at Hill AFB, a metal surface that is rendered non-reflective by a rough surface profile is not well suited to analysis by grazing-angle reflectance. Grazing-angle reflectance FTIR is unsuitable for these types of materials.

Inorganic surface contaminants, such as rust or scale, were not evaluated. The FTIR technique is capable of detecting a number of metal oxides, but analysis is complicated by the lack of available data on the optical properties of these materials. Additionally, the preparation of accurate calibration standards would be extremely difficult due to a lack of solubility for these materials.

b. A significant need exists in the military's cleaning applications for the determination of specific minimum acceptable contamination levels for each unique process.

Testing of the grazing-angle device has shown that the FTIR device possesses a detection level of around 0.22 $\mu g/cm^2$ for many hydrocarbon contaminants. Since coating failures may occur only at higher residual contamination levels, indiscriminant use of the technique could lead to over cleaning of component surfaces. That is, inspections with the FTIR instrument could actually lead shop personnel to over clean their parts since the device is much more sensitive to contaminants than water break testing. Therefore, a critical step in the application of the FTIR monitoring technique for each unique cleaning application is the determination of acceptable contamination levels, i.e., a pass / fail criteria to determine "how clean is clean enough" for that particular cleaning process to mitigate instrument-driven over cleaning. This might be accomplished by lap-shear tests on calibrated coupons, or by some other means. Once the threshold is established for a particular process, the FTIR software will be able to indicate whether the surface being analyzed is below or above the threshold and by how much.

In a shop environment, knowing the film thickness of the contaminant on a component's surface allows the analyst to make decisions to implement or change a cleaning process. A process that over-cleans its parts is a waste of resources, time, and money. A process that under-cleans may result in a costly and subsequent serious part or assembly failure.

Depending on the part's function, required cleanliness levels will vary. Sub-micrometer detection, for example, would be essential for determining low levels of silicone on aircraft parts. New mandatory low volatile organic content (VOC) coatings used on aircraft skins are very sensitive to silicone contaminants. These contaminants are known to leach out of door and window seals. The low levels would not be visible to the naked eye but may still require removal to prevent disbonding of the coating. Since recoating an aircraft is extremely expensive (roughly $80K to strip and $90K to recoat a C-130 aircraft), detection of the contamination beforehand is a wise approach.

c. Although an upgraded portable FTIR device was developed with user-friendly features, FTIR technology is still viewed as too complex by non-technical repair and maintenance personnel, preventing it from being implemented to its full potential in DOD cleanliness verification applications.

The portable grazing-angle reflectance device has developed into a commercially available item and has been purchased by both commercial and Government facilities. Nevertheless, DOD facilities have not, as of the time of this report, purchased and implemented the technology into their cleaning processes. During the course of the project, SERDP project members observed a reticence among shop maintenance and repair personnel to accept a tool that requires calibration, or likewise, a cursory understanding of infrared spectroscopy.

A much more common detection method used in military depots is "hexane extraction." A surface of interest is swabbed with a hexane soaked applicator, and then the dissolved surface contaminants are extracted from the solvent and analyzed. Although this detection method also involves calibration of an instrument, the calibration step is performed in an off-site laboratory by personnel specifically trained in spectroscopy or chromatography.

At each facility visited by the project team members, however, there were always technical personnel on-site or at the activities working with the shop and depot technicians. Among technical personnel, there was a general resistance to change and a desire to continue using "tried and true" methods. Some have seen other promising prototype devices come and go and have developed a skeptical attitude towards any new device.

Additionally, having to prepare calibration coupons for a cleaning verification method may present a challenge. As indicated in Section A of this report, achieving uniform, utrathin films requires special expertise and equipment. If the surface in question must have contamination levels < 10 $\mu g/cm^2$, the coupons will likely need to be prepared by an outside organization. Depending on the contaminant though, these coupons could be stable for months if properly handled, eliminating the need for frequent purchase of preparing calibration specimens.

Finally the problem of contaminant matrices may lead personnel to reject the FTIR as a viable method. If the surface in question contains more than one contaminant, and no one contaminant is dominant in concentration, an accurate calibration would require the matrix to be duplicated in the reference coupons. This requires more knowledge about the contaminant matrix composition.

With time, it is anticipated that the increasing user-base for the portable grazing-angle FTIR device will lead to method developments that will make it easier for new users to utilize the technology for their field cleaning verification needs. With continuing increase in popularity, the manufacturer will likely keep implementing improvements to the system, making it more desirable to the DOD community.

6. ACKNOWLEDGEMENTS

This work was sponsored by the U.S. Department of Defense Strategic Environmental Research and Development Program (SERDP). The author gratefully acknowledges Drs. David Ottesen and Shane Sickafoose of Sandia National Laboratories for providing their expertise and integral support to NFESC's portion of the project. The author also gratefully acknowledges the personnel from NADEP North Island and Hill AFB who generously offered their technical expertise and depot applications for demonstration of the portable grazing-angle FTIR.

7. REFERENCES

1. NFESC Technical Memorandum TM-2335-SHR, "Grazing-Angle Fourier Transform Infrared Spectroscopy for Online Surface Cleanliness Verification: Year 1," by T. A. Hoffard, et. al, Naval Facilities Engineering Service Center, July 2000.

2. Francis, S.A., and Ellison, A.H., J. Opt Soc. Am., 49, 131, 1959.

3. Greenler, R.G.J., "Infrared Study of Adsorbed Molecules on Metal Surfaces by Reflection Techniques." J. Chem. Phys., 44(1), 310-15, 1966.

4. Smith, B.C., Fundamentals of Fourier Transform Infrared Spectroscopy, CRC Press LLC, 1996.

5. Ulman, A., Ed. Characterization of Organic Thin Films, Materials Characterization Series, Butterworth-Heinemann, Stoneham MA, 1995.

6. Ferraro, J.R. and Basile, L.J., Ed. Fourier Transform Infrared Spectroscopy – Applications to Chemical Systems, Vol. 4, Academic Press, Inc., New York, 1985.

7. "External Reflectance Spectroscopy of Surfaces," Spectra-Tech FT-IR Technical Note TN-3, SpectaTech, Inc., 1998.

8. Ottesen, D., et al., "Cleaning Verification Monitor Technique Based on Infrared Optical Methods," FY1999 Annual Report, Strategic Environmental Research and Development Program, Project PP-1138, December 1999.

9. Griffiths, P.R. and de Haseth, J.A., Fourier Transform Infrared Spectrometry, Chemical Analysis Vol. 83, John Wiley & Sons, New York, 1986.

APPENDIX A

Matrix of Calibrated Samples for Grazing-angle Reflectance FTIR Testing

Years 2 -3

Sample ID	Geometry	Substrate	Contaminant	Surface Roughness	Residue Weight (gm)	Estimated Film Thickness* (µm)	Estimated Concentration (µg/cm^2)
428	1.5" x 5" flat panel	Aluminum 7075-T6	D	600 grit	0.00674	1.2549	139.3
429	1.5" x 5" flat panel	Aluminum 7075-T6	D	600 grit	0.00572	1.0650	118.2
430	1.5" x 5" flat panel	Aluminum 7075-T6	D	600 grit	0.00508	0.9458	105.0
431	1.5" x 5" flat panel	Aluminum 7075-T6	D	600 grit	0.00258	0.4804	53.3
432	1.5" x 5" flat panel	Aluminum 7075-T6	D	600 grit	0.00134	0.2495	27.7
018	1.5" x 5" flat panel	Aluminum 7075-T6	D	220 grit	0.00527	0.9812	108.9
019	1.5" x 5" flat panel	Aluminum 7075-T6	D	220 grit	0.00208	0.3873	43.0
020	1.5" x 5" flat panel	Aluminum 7075-T6	D	220 grit	0.00502	0.9347	103.7
021	1.5" x 5" flat panel	Aluminum 7075-T6	D	220 grit	0.00845	1.5733	174.6
022	1.5" x 5" flat panel	Aluminum 7075-T6	D	220 grit	0.00146	0.2718	30.2
215	1.5" x 5" flat panel	Aluminum 7075-T6	D	80 grit	0.00489	0.9105	101.0
216	1.5" x 5" flat panel	Aluminum 7075-T6	D	80 grit	0.00164	0.3053	33.9
217	1.5" x 5" flat panel	Aluminum 7075-T6	D	80 grit	0.00525	0.9775	108.5
218	1.5" x 5" flat panel	Aluminum 7075-T6	D	80 grit	0.01251	2.3292	258.5
219	1.5" x 5" flat panel	Aluminum 7075-T6	D	80 grit	0.00149	0.2774	30.8
Ti5-11	1.5" x 5" flat panel	Titanium 6Al	D	600 grit	0.01073	1.9978	221.7
Ti5-12	1.5" x 5" flat panel	Titanium 6Al	D	600 grit	0.00576	1.0724	119.0
Ti5-13	1.5" x 5" flat panel	Titanium 6Al	D	600 grit	0.00415	0.7727	85.7
Ti5-14	1.5" x 5" flat panel	Titanium 6Al	D	600 grit	0.00141	0.2625	29.1

Sample ID	Geometry	Substrate	Contaminant	Surface Roughness	Residue Weight (gm)	Estimated Film Thickness* (µm)	Estimated Concentration (µg/cm^2)
Ti5-05	1.5” x 5” flat panel	Titanium 6Al	D	600 grit	0.00141	0.2625	29.1
Ti5-31	1.5” x 5” flat panel	Titanium 6Al	D	220 grit	0.01056	1.9661	218.2
Ti5-32	1.5” x 5” flat panel	Titanium 6Al	D	220 grit	0.00482	0.8974	99.6
Ti5-33	1.5” x 5” flat panel	Titanium 6Al	D	220 grit	0.00574	1.0687	118.6
Ti5-34	1.5” x 5” flat panel	Titanium 6Al	D	220 grit	0.00149	0.2774	30.8
Ti5-46	1.5” x 5” flat panel	Titanium 6Al	D	220 grit	0.00139	0.2588	28.7
304-31S	1.5” x 5” flat panel	Stainless Steel 304	D	600 grit	0.0076	1.4150	157.0
304-32S	1.5” x 5” flat panel	Stainless Steel 304	D	600 grit	0.00498	0.9272	102.9
304-33S	1.5” x 5” flat panel	Stainless Steel 304	D	600 grit	0.00523	0.9738	108.1
304-34S	1.5” x 5” flat panel	Stainless Steel 304	D	600 grit	0.00159	0.2960	32.9
304-45S	1.5” x 5” flat panel	Stainless Steel 304	D	600 grit	0.00128	0.2383	26.4
304-31R	1.5” x 5” flat panel	Stainless Steel 304	D	220 grit	0.01087	2.0238	224.6
304-32R	1.5” x 5” flat panel	Stainless Steel 304	D	220 grit	0.00581	1.0817	120.0
304-33R	1.5” x 5” flat panel	Stainless Steel 304	D	220 grit	0.00501	0.9328	103.5
304-34R	1.5” x 5” flat panel	Stainless Steel 304	D	220 grit	0.00146	0.2718	30.2
304-49R	1.5” x 5” flat panel	Stainless Steel 304	D	220 grit	0.00128	0.2383	26.4
C4340-21S	1.5” x 5” flat panel	Steel Alloy 4340	D	600 grit	0.0104	1.9363	214.9
C4340-22S	1.5” x 5” flat panel	Steel Alloy 4340	D	600 grit	0.0062	1.1544	128.1
C4340-23S	1.5” x 5” flat panel	Steel Alloy 4340	D	600 grit	0.0058	1.0799	119.8
C4340-24S	1.5” x 5” flat panel	Steel Alloy 4340	D	600 grit	0.003	0.56	62.0
C4340-45S	1.5” x 5” flat panel	Steel Alloy 4340	D	600 grit	0.0012	0.2234	24.8
C4340-21R	1.5” x 5” flat panel	Steel Alloy 4340	D	220 grit	0.0095	1.7688	196.3
C4340-22R	1.5” x 5” flat panel	Steel Alloy 4340	D	220 grit	0.0054	1.0054	111.6
C4340-23R	1.5” x 5” flat panel	Steel Alloy 4340	D	220 grit	0.0013	0.2420	26.9

Sample ID	Geometry	Substrate	Contaminant	Surface Roughness	Residue Weight (gm)	Estimated Film Thickness* (µm)	Estimated Concentration (µg/cm^2)
C4340-24R	1.5" x 5" flat panel	Steel Alloy 4340	D	220 grit	0.0058	1.0799	119.8
C4340-47R	1.5" x 5" flat panel	Steel Alloy 4340	D	220 grit	0.0008	0.1489	16.5
FlexAl-1	1-cm radius cylinder	Flexible Aluminum sheet	D	Smooth	0.00729	1.3573	150.6
FlexAl-2	1-cm radius cylinder	Flexible Aluminum sheet	D	Smooth	0.00474	0.8825	97.9
FlexAl-3	1-cm radius cylinder	Flexible Aluminum sheet	D	Smooth	0.00166	0.3091	34.3
FlexAl-4	1-cm radius cylinder	Flexible Aluminum sheet	D	Rough	0.00905	1.6850	187.0
FlexAl-5	1-cm radius cylinder	Flexible Aluminum sheet	D	Rough	0.00506	0.9421	104.5
FlexAl-6	1-cm radius cylinder	Flexible Aluminum sheet	D	Rough	0.00163	0.3035	33.7
462	1.5" x 5" flat panel	Aluminum 7075-T6	B	600 grit	0.00079	0.215	16.3
463	1.5" x 5" flat panel	Aluminum 7075-T6	A	600 grit	0.00189	0.421	39.0
464	1.5" x 5" flat panel	Aluminum 7075-T6	D	600 grit	0.00051	0.095	10.5
465	1.5" x 5" flat panel	Aluminum 7075-T6	C	600 grit	0.00172	0.361	35.5
220	1.5" x 5" flat panel	Aluminum 7075-T6	B	220 grit	0.00049	0.133	10.1
221	1.5" x 5" flat panel	Aluminum 7075-T6	A	220 grit	0.00170	0.379	35.1
222	1.5" x 5" flat panel	Aluminum 7075-T6	D	220 grit	0.00078	0.145	16.1
223	1.5" x 5" flat panel	Aluminum 7075-T6	C	220 grit	0.00352	0.661	72.7
ALED1	1.5" x 5" flat panel	Aluminum 7075 Etched & Deoxidized	North Island Soil Mix	Approx. 400 grit	0.00029	0.06	6.0
ALED2	1.5" x 5" flat panel	Aluminum 7075 Etched & Deoxidized	North Island Soil Mix	Approx. 400 grit	0.00085	0.17	17.6
ALED3	1.5" x 5" flat panel	Aluminum 2024 Etched & Deoxidized	North Island Soil Mix	Approx. 400 grit	0.00061	0.13	12.6

Sample ID	Geometry	Substrate	Contaminant	Surface Roughness	Residue Weight (gm)	Estimated Film Thickness* (µm)	Estimated Concentration (µg/cm^2)
ALED4	1.5" x 5" flat panel	Aluminum 2024 Etched & Deoxidized	North Island Soil Mix	Approx. 400 grit	0.00079	0.16	16.3
ALCC1	1.5" x 5" flat panel	Aluminum 2024 Chromate Conversion Coated	North Island Soil Mix	Approx. 400 grit	0.00036	0.07	7.4
ALCC2	1.5" x 5" flat panel	Aluminum 2024 Chromate Conversion Coated	North Island Soil Mix	Approx. 400 grit	0.00102	0.21	21.1
ALAD1	1.5" x 5" flat panel	Aluminum 2024 Type II Sulfuric Acid Anodized	North Island Soil Mix	Approx. 400 grit	0.00060	0.12	12.4
ALAD2	1.5" x 5" flat panel	Aluminum 2024 Type II Sulfuric Acid Anodized	North Island Soil Mix	Approx. 400 grit	0.00068	0.14	14.0
ED5	1.5" x 5" flat panel	Aluminum 7075 Etched & Deoxidized	North Island Soil Mix	Approx. 400 grit	0.00270	0.625	55.8
ED6	1.5" x 5" flat panel	Aluminum 7075 Etched & Deoxidized	North Island Soil Mix	Approx. 400 grit	0.00100	0.231	20.7
ED7	1.5" x 5" flat panel	Aluminum 7075 Etched & Deoxidized	North Island Soil Mix	Approx. 400 grit	0.00140	0.324	28.9
ED8	1.5" x 5" flat panel	Aluminum 7075 Etched & Deoxidized	North Island Soil Mix	Approx. 400 grit	0.00050	0.116	10.3
ED9	1.5" x 5" flat panel	Aluminum 2024 Etched & Deoxidized	North Island Soil Mix	Approx. 400 grit	0.00210	0.486	43.4
ED10	1.5" x 5" flat panel	Aluminum 2024 Etched & Deoxidized	North Island Soil Mix	Approx. 400 grit	0.00109	0.252	22.5
ED11	1.5" x 5" flat panel	Aluminum 2024 Etched & Deoxidized	North Island Soil Mix	Approx. 400 grit	0.00153	0.354	31.6
ED12	1.5" x 5" flat panel	Aluminum 2024 Etched & Deoxidized	North Island Soil Mix	Approx. 400 grit	0.00055	0.127	11.4
CC3	1.5" x 5" flat panel	Aluminum 7075 Chromate Conversion Coated	North Island Soil Mix	Approx. 400 grit	0.00196	0.454	40.5

Sample ID	Geometry	Substrate	Contaminant	Surface Roughness	Residue Weight (gm)	Estimated Film Thickness* (µm)	Estimated Concentration (µg/cm^2)
CC4	1.5” x 5” flat panel	Aluminum 7075 Chromate Conversion Coated	North Island Soil Mix	Approx. 400 grit	0.00136	0.315	28.1
CC5	1.5” x 5” flat panel	Aluminum 7075 Chromate Conversion Coated	North Island Soil Mix	Approx. 400 grit	0.00271	0.627	56.0
CC6	1.5” x 5” flat panel	Aluminum 7075 Chromate Conversion Coated	North Island Soil Mix	Approx. 400 grit	0.00069	0.160	14.3
CC7	1.5” x 5” flat panel	Aluminum 2024 Chromate Conversion Coated	North Island Soil Mix	Approx. 400 grit	0.00271	0.627	56.0
CC8	1.5” x 5” flat panel	Aluminum 2024 Chromate Conversion Coated	North Island Soil Mix	Approx. 400 grit	0.00115	0.266	23.8
CC9	1.5” x 5” flat panel	Aluminum 2024 Chromate Conversion Coated	North Island Soil Mix	Approx. 400 grit	0.00149	0.345	30.8
CC10	1.5” x 5” flat panel	Aluminum 2024 Chromate Conversion Coated	North Island Soil Mix	Approx. 400 grit	0.00060	0.139	12.4
AD3	1.5” x 5” flat panel	Aluminum 2024 Type II Sulfuric Acid Anodized	North Island Soil Mix	Approx. 400 grit	0.00259	0.599	53.5
AD4	1.5” x 5” flat panel	Aluminum 2024 Type II Sulfuric Acid Anodized	North Island Soil Mix	Approx. 400 grit	0.00099	0.229	20.5
AD5	1.5” x 5” flat panel	Aluminum 2024 Type II Sulfuric Acid Anodized	North Island Soil Mix	Approx. 400 grit	0.00363	0.840	75.0
AD6	1.5” x 5” flat panel	Aluminum 2024 Type II Sulfuric Acid Anodized	North Island Soil Mix	Approx. 400 grit	0.00079	0.183	16.3
346	1.5” x 5” flat panel	Aluminum 70705	North Island Soil Mix	400 grit	0.00087	0.201	18.0
347	1.5” x 5” flat panel	Aluminum 70705	North Island Soil Mix	400 grit	0.00106	0.245	21.9
348	1.5” x 5” flat panel	Aluminum 70705	North Island Soil Mix	400 grit	0.00231	0.534	47.7
349	1.5” x 5” flat panel	Aluminum 70705	North Island Soil Mix	400 grit	0.00527	1.219	108.9
Anod-1	1.5” x 5”	Chromic Anodized	North Island Soil	Approx. 400 grit	0.00032	0.074	6.6

Sample ID	Geometry	Substrate	Contaminant	Surface Roughness	Residue Weight (gm)	Estimated Film Thickness* (µm)	Estimated Concentration (µg/cm^2)
	flat panel	Al-7075	Mix				
Anod-2	1.5” x 5” flat panel	Chromic Anodized Al-7075	North Island Soil Mix	Approx. 400 grit	0.00048	0.111	9.9
Anod-3	1.5” x 5” flat panel	Chromic Anodized Al-7075	North Island Soil Mix	Approx. 400 grit	0.00186	0.430	38.4
Anod-4	1.5” x 5” flat panel	Chromic Anodized Al-7075	North Island Soil Mix	Approx. 400 grit	0.00374	0.865	77.3
Aldn-1	1.5” x 5” flat panel	Dichromate Alodyne Al-7075	North Island Soil Mix	Approx. 400 grit	0.00047	0.109	9.7
Aldn-2	1.5” x 5” flat panel	Dichromate Alodyne Al-7075	North Island Soil Mix	Approx. 400 grit	0.00014	0.032	2.9
Aldn-3	1.5” x 5” flat panel	Dichromate Alodyne Al-7075	North Island Soil Mix	Approx. 400 grit	0.00183	0.423	37.8
Aldn-4	1.5” x 5” flat panel	Dichromate Alodyne Al-7075	North Island Soil Mix	Approx. 400 grit	0.00483	1.118	99.8
350	1.5” x 5” flat panel	Aluminum 70705	Methyl-methacrylate blast media	400 grit	0.00138	0.248	28.5
352	1.5” x 5” flat panel	Aluminum 70705	Methyl-methacrylate blast media	400 grit	0.00073	0.131	15.1
351	1.5” x 5” flat panel	Aluminum 70705	Methyl-methacrylate blast media	400 grit	0.00106	0.190	21.9
353	1.5” x 5” flat panel	Aluminum 70705	Methyl-methacrylate blast media	400 grit	0.00503	0.904	103.9
Anod-5	1.5” x 5” flat panel	Chromic Anodized Al-7075	Methyl-methacrylate blast media	Approx. 400 grit	0.00224	0.402	46.3
Anod-6	1.5” x 5” flat panel	Chromic Anodized Al-7075	Methyl-methacrylate blast media	Approx. 400 grit	0.00315	0.566	65.1
Anod-7	1.5” x 5” flat panel	Chromic Anodized Al-7075	Methyl-methacrylate blast media	Approx. 400 grit	0.00219	0.393	45.2
Anod-8	1.5” x 5” flat panel	Chromic Anodized Al-7075	Methyl-methacrylate blast media	Approx. 400 grit	0.00479	0.861	99.0
Aldn-5	1.5” x 5” flat panel	Dichromate Alodyne Al-7075	Methyl-methacrylate blast media	Approx. 400 grit	0.00179	0.322	37.0

Sample ID	Geometry	Substrate	Contaminant	Surface Roughness	Residue Weight (gm)	Estimated Film Thickness* (µm)	Estimated Concentration (µg/cm^2)
Aldn-6	1.5" x 5" flat panel	Dichromate Alodyne Al-7075	Methyl-methacrylate blast media	Approx. 400 grit	0.00173	0.311	35.7
Aldn-7	1.5" x 5" flat panel	Dichromate Alodyne Al-7075	Methyl-methacrylate blast media	Approx. 400 grit	0.00074	0.133	15.3
Aldn-8	1.5" x 5" flat panel	Dichromate Alodyne Al-7075	Methyl-methacrylate blast media	Approx. 400 grit	0.00688	1.236	142.1

*Based on specific gravity of oven-dried sample of contaminant

A:	0.93 gm/cc
B:	0.76 gm/cc
C:	1.1 gm/cc
D:	1.1 gm/cc
North Island Soil Mix:	0.89 gm/cc
Hill Plastic Blast Media	1.15 gm/cc